Joint Centre for Mesoscale Meteorology, Reading, UK

Structure of a midlatitude cyclone before occlusion

K. A. Browning
N. Roberts

Internal Report No. 5

July 1993

Met Office Joint Centre for Mesoscale Meteorology Department of Meteorology
University of Reading PO Box 243 Reading RG6 6BB United Kingdom
Tel: +44 (0)118 931 8425 Fax: +44 (0)118 931 8791
www.metoffice.com

Structure of a midlatitude cyclone before occlusion

K A Browning and N Roberts

Joint Centre for Mesoscale Meteorology*
University of Reading, UK

* The Joint Centre for Mesoscale Meteorology is supported by the Meteorological Office and the University of Reading, Department of Meteorology

Summary

A diagnostic study of a mid-latitude cyclone has been carried out using routinely available NWP model products and imagery. The cyclone was intense but not exceptionally so, and the results are believed to have some generality. The detailed description of the cyclone structure just before occlusion integrates concepts from a number of researchers into a common framework. A dominant feature of the cyclone, close to its centre, was a 'hook cloud' - a smaller version of what is often referred to as a 'cloud head'. The hook cloud was caused by two flows which entered it from the east, ascending and fanning out within it. One flow brought low-θ_w air into the hook cloud from low levels ahead of the warm front (the 'cold conveyor belt'). The other flow was due to high-θ_w air that peeled off from the base of the main warm sector airflow (ie. part of the 'warm conveyor belt') and travelled in the boundary layer towards the cyclone centre, first undercutting dry air that had earlier descended from the upper troposphere (called a 'dry intrusion'), and then ascending at the upper boundary of the hook cloud, above the cold conveyor belt. The transverse circulation that gave the ascent within the hook cloud also led to the cold front fracturing along its length into two separate sharp surface cold fronts, with a more diffuse frontal region in between (a so-called 'frontal fracture'). The two sharp surface cold fronts were associated with narrow cold frontal rainbands ('line convection'), one of the line convection segments forming the southern edge of the hook cloud. The overrunning of the dry intrusion in the region of frontal fracture led to a structure (known as a 'split front') in which an upper level humidity front began to run ahead of the position of the surface cold front. A notable feature of the cyclone structure at this intermediate stage in its evolution was that a large proportion of the system's precipitation was being generated by ascent of relatively cold air (the cold conveyor belt) in the hook cloud as part of an indirect thermal circulation at the left exit of an upper level jet.

1. Introduction

There has been much research recently into the structure and dynamics of extratropical cyclones, especially rapidly deepening cyclones. A review of advances in understanding brought about by a combination of theoretical, observational and modelling approaches was published following the Palmén Memorial Symposium (eds., Newton and Holopainen 1990). The present study develops some of the ideas on cyclone and frontal structure presented by the various authors in that review and it complements ideas developed by Bader et al (1993) in their imagery interpretation manual. The intention is to describe a moderately intense cyclone of a kind likely to be encountered more commonly than the extreme cases often selected for study.

The raw material for our study was obtained from the diagnosis of a mid-latitude cyclone using analysis and 3-h forecast output from 6-hourly runs of the limited-area version of the Meteorological Office's Unified Model together with surface observations and imagery from METEOSAT and the UK Weather Radar Network. The cyclone at the time of most detailed analysis was over the data-rich British Isles and this was reflected in the model performance. Within the limitations of the model resolution (50 km grid), the fit between the above model products and aspects of the imagery was reassuringly close (Sec. 3). Although the cyclone studied was not large and did not (quite) undergo 'explosive' cyclogenesis according to the definition (24 mb in 24h) of Sanders and Gyakum (1980), it nevertheless possessed (in a less striking fashion) many of the characteristics of major cyclones as

described, for example, by Uccellini (1990). Indeed it gave rise to some damaging winds with surface gusts in excess of 35m s^{-1} over southern England during the period of the study. The cyclone structure during its pre-occlusion phase was captured particularly well as it crossed the British Isles and it has been possible to undertake a fairly detailed analysis of its structure at this time (Sec 3) using routinely available data.

The study synthesizes a number of existing concepts and develops a simple scheme for synoptic analysis. The concepts to be synthesized are as follows:

- 'Warm conveyor belt' (Harrold 1973) - a rather well defined, and often the main rain-producing, flow of high wet-bulb potential temperature (θ_w) within mid-latitude frontal systems.

- 'Cold conveyor belt' (Carlson 1980) - air ahead of and beneath the warm front which, relative to the advancing system, flows rapidly rearwards around the north side of the low centre.

- 'Dry intrusion' - a stream of air from the upper troposphere and lower stratosphere (Reed and Danielsen 1959) which, after earlier descent, approaches the centre of the cyclone as a well defined reascending dry flow with low θ_w (Young et al 1987). Its leading edge produces what McBean and Stewart (1991) call an 'upper-level moisture front' and Mass and Schultz (1993) call an 'upper-level humidity front'.

- 'Dry slot' (Weldon 1979, Weldon and Holmes 1991) - a satellite-detected, almost cloud-free, zone indicative of the dry intrusion approaching the centre of a developing cyclone.

- 'Hook cloud' - we use this term to describe the hook-shaped cloud feature on the poleward side of the dry slot associated with a region of slantwise ascent poleward of the main polar front cloud band. Large hook clouds with sharp poleward boundaries are referred to as 'cloud heads' (Bottger et al 1975, Shutts 1990). In the later stages of cyclone development, cloud at the tip of the hook circulates around the cyclone centre: this had not (quite) begun at the stage of evolution investigated in this paper.

- 'Line convection' (Browning and Harrold 1970) - a rather two-dimensional strip of forced convection leading to a narrow band of rain echo of small vertical extent, aligned along a sharp surface cold front, often segmented into line elements separated by very small gaps (Hobbs and Biswas 1979) and occasionally also by a large gap or 'step' (James and Browning 1979).

- 'Frontal fracture' (Shapiro and Keyser 1990) - a horizontal break or dislocation in the structure of a sharp cold frontal transition occurring close to the centre of a developing cyclone (a large version of the 'step' described by James and Browning (1979)).

- 'Split front' (Browning and Monk 1982) - a vertical break in the structure of a cold front in which low-θ_w air aloft overruns moist high-θ_w air to give an 'upper cold front' (moisture front) ahead of the surface cold front corresponding to the 'upper-level humidity front' of Mass and Schultz (1993).

2. Broad-scale evolution

The cyclone to be studied developed ahead of a mobile broad upper trough (Fig 1). A small closed circulation was first identified at the surface at 06 UTC on 12 January 1993. It then deepened steadily, according to the model, from 1010 mb at 12/12Z (Fig 2(a)), to 988 mb when it was over England at 13/15Z (Fig 2(b)), and further to 973 mb by the time it reached the Gulf of Finland at 14/09Z. It was a secondary wave depression on the southern flank of a very large low-pressure area and much of its deepening was due to it moving closer to the main low-pressure area. In fact its depth expressed in terms of its own closed isobars was consistently only 2 to 4 mb except after 13/18Z when a period of rapid deepening and occlusion set in. This rapid deepening is mentioned again later but is peripheral to our main theme which is the structure of the cyclone just before the onset of rapid deepening and occlusion.

The sequence of mainly 6-hourly satellite images in Fig 3 shows the evolution of the cloud associated with the developing cyclone and sets the scene for the detailed analysis in Sec. 3. The evolving pattern is consistent with the conceptual model of Weldon (1979), reproduced as Fig 1 in Young et al (1987), in which a 'baroclinic leaf cloud' develops a convex-poleward bulge which is penetrated by a relatively cloud-free 'dry slot', with a hook shaped cloud appearing on its poleward side. This 'hook cloud' is similar to what Bottger et al (1975) and others refer to as a 'cloud head'. The sequences of model products in Figs 4, 5 and 6, covering almost the same set of space-time windows as in Fig 3, show key dynamical features describing the evolution of the cyclone. They are all 3-h forecasts but are not inconsistent with or noticeably inferior to the sequence of model analyses; indeed they should be dynamically more balanced. Important relationships to note are:

- The cyclone developed initially beneath the right entrance region of a developing upper jet streak (J_1 in Fig 4). The jet streak itself was collocated with the area of high cloud associated with slantwise ascent just to the north of the developing cyclone (compare Figs 3 and 4). As the cyclone developed, a dual jet streak structure formed in the characteristic manner described by McCallum and Norris (1990) (see their Fig 4): J_1 continued to be fed by the slantwise ascent from the cyclone whilst, in the tail of the jet upwind of the cyclone, the winds aloft strengthened to form a new jet streak (J_2) with the cyclone at its left exit (Fig 4).

- A warm conveyor belt was defined clearly at low levels by a strip of high θ_w and strong winds (Fig 5(a)) which intensified as the cyclone developed. The warm conveyor belt was accompanied initially by a developing strip of high potential vorticity (PV) at 900 mb (Fig 5(b)), associated with convective clouds and diabatic production of PV (Thorpe and Emanuel 1985). The cyclone developed at the northern edge of the PV strip; the 900 mb PV increased with time at the location of the cyclone whilst the rest of the PV strip, and the ascent and condensation responsible for it, eventually withered away (Fig 5(b)). Near the position of the cyclone centre, the leading (northern) edge of the high-θ_w flow turned cyclonically (Fig 5(a)) and it terminated at low levels with the ascent of warm conveyor belt air within the hook cloud (Sec. 3). This was part of the ageostrophic transverse circulation at the exit of new jet streak J_2 which played an important role in the cyclone structure as described in Sec. 3 (see also Uccellini and Johnson 1979).

- The height of the tropopause decreased, as one would expect, on the cold side of the upper jet but, in particular, there was a region of locally even lower tropopause just to the west of the developing cyclone which can be seen edging closer to it throughout the sequence. This is shown in Fig 6 by the plots of the PV=2 surface, which corresponds to the dynamical tropopause (Hoskins et al 1985). Note especially the 7.5 km contour for PV=2 (Fig 6) encroaching upon the low-level PV maximum (Fig 5(b)), and reaching a state of near-vertical alignment by 13/21Z. This was presumably the cause of the development of upper-level jet J_2. Already by 13/15Z the leading edge of the region of low tropopause was almost overhead of the low-level PV maximum associated with the cyclone and the winds in the associated jet J_2 had intensified to 70 m s^{-1}. This is the stage for which we conduct a detailed analysis of the cyclone structure (Sec. 3); shortly afterwards the cyclone entered a period of more rapid cyclogenesis and occlusion due to the coupling of the upper and low-level PV maxima, but this will not be discussed in this paper.

3. Detailed structure at 15 UTC, 13 January.

(a) Hook cloud and dry slot.

The zoomed satellite infra-red imagery in Fig 7(a) shows the hook cloud at 15 UTC, 13 January extending from the southern Irish Sea across northern Britain into the North Sea. A dry slot intruding from SW England to the Humber estuary on the east coast of England, separates the hook cloud from the polar front cloud band which trails out of the picture to the south. As is usual for hook clouds, the height of the cloud tops rises steadily away from its southern edge, near the dry slot. There was extensive rain associated with a large part of the hook cloud (Fig 7(b)). Much of the heaviest rain was produced by the region of shallow cloud towards the southern part of the hook cloud which, from the bright, lumpy appearance of the visible imagery (not shown) and the radar echo, was evidently convective. Fig 7(c) clarifies the relationship between the cloud and rain at 15 UTC. The wide arrow in this figure also shows schematically the model-derived extent and relative motion of the dry intrusion responsible for the dry slot.

(b) Line convection segments separated by a large gap as evidence of frontal fracture.

Figure 7(d) shows the model-derived surface 'analysis' with fronts superimposed as obtained from a careful reanalysis of observations. The frontal analysis in Fig 7(d) differs from the Met Office's Central Forecast Office analysis by taking account of the observed gap in the cold front over the Channel. Attention was first drawn to this split by the radar rainfall pattern (Fig 7(b)) which showed two narrow cold frontal rainbands indicative of line convection at a sharp surface cold front (Browning and Harrold 1970). One of these was situated along the southeastern boundary of the hook cloud. The other, quite separate one, was situated over Brittany and part of the Channel. The Unified Model did not fully resolve this gap; however, the S-shape of the model-derived θ_w contours (see the $\theta_w = 11°C$ curve in Fig 7(d)), whilst underestimating the gap, does still show some tendency to fit the two cold front segments. The dashed curve in Fig 7(d) shows the authors' inference as to what the 11°C isopleth should have been; the 10°C isopleth should be redrawn in a similar manner. This is consistent with the analysis of observed θ_w shown in Fig 7(e). (The agreement

between the model-derived and observed θ_w is otherwise generally quite good near and on the warm side of the fronts. However, on the cold side over Wales and northern England the model failed to reproduce observed low values which may have been caused by latent heat sinks within the precipitation area).

A major break between two segments of line convection, as observed here, corresponds to a particularly large version of what James and Browning (1979) referred to as a large gap or step. As shown by their schematic model of a cold frontal transition zone (see their Fig 8), a surface front is sharp where there is line convection but diffuse (and dry) in the region of a large gap. In the specific context of a developing cyclone this feature corresponds to the frontal fracture described by Shapiro and Keyser (1990, eg their Fig 10.14b) and Neiman et al (1993, eg their Fig 3a). The frontal fracture developed in association with the ageostrophic transverse circulation at the exit of the 300 mb jet whose core was centred just 50 km north of Brest at this time (see J_2 in Fig 4). The transverse circulation was transporting high-θ_w air towards the northwest in the boundary layer (Fig 7(d)) before it ascended within the hook cloud. This was also shown in Fig 5(a) by the small but significant turning (after 13/03Z) of the axis of maximum θ_w towards the developing cyclone; it is also shown by the relative flow in the θ_w = 11°C surface as part of the analysis described next (Fig 8).

(c) Warm conveyor belt flow with its lower part peeling off to feed upper part of the hook cloud.

Fig 8 depicts an analysis of relative flow within moist isentropic surfaces to account for the shape of the pattern of cloud and the associated rainfall production. Fig 8(a) is an example of the raw computer output from which have been derived the detailed analyses for individual θ_w-surfaces shown in the other parts of Fig 8, viz: θ_w = 11°C in Fig 8(b), 10° in Fig 8(c), 9° in Fig 8(d) and 12° in Fig 8(e). Also shown in Fig 8(e) is a synthesis of all these flows, specifically to show the 9, 10 and 11° flows emerging into the hook cloud from underneath the 12° flow. The nature of the 9, 10 and 11° flows will be discussed later in Sec 3(d): first we consider the relationship between the 11 and 12° flows originating in the warm sector.

The 12°C flow (see right-hand part of Fig 8(e)) was within the main warm conveyor belt flow (W1) along the axis of the polar front cloud band. The 11°C flow (W2 in Fig 8(b)) corresponds to air that originated in the same warm conveyor belt but which, over SE England in the vicinity of the cyclone centre, peeled off towards the west to form a portion of the upper part of the hook cloud. Ahead of the surface cold front the 11° air was within the planetary boundary layer. Here frictional retardation and turning can account for its relative flow being directed with a component rearwards against the main warm conveyor belt flow plus a component towards the surface cold front. However, the enhanced component of the 11°C flow towards the surface cold front was associated with the transverse ageostrophic circulation at the exit of jet J_2 (Fig 7(d)). The notion of the peeling off of W2 from the base of the main warm conveyor belt W1 was introduced by Young et al (1987) and developed by Young (1989) and Bader et al (1993, see schematics in their Sec 5.2) who stressed the importance of the ageostrophic transverse circulation at the jet exit in generating W2 and the associated hook cloud. (Note that Young et al (1987) referred to W2 as W1 and vice versa, although the later articles adopted the present notation). A similar airflow pattern

was also shown by McGinnigle et al (1988) for the mature stage of an instant occlusion, but the origin of W2 in their case appears to have been tied to the region ahead of a pre-existing secondary cold front on the poleward side of the main polar front zone. There were two separate cold front segments in the present case, too, (Fig 7(d)), but this was due to the deformation or fracture of a single frontal zone as described by Shapiro and Keyser (1990). Shapiro and Keyser actually refer to the cold front segment bounding the hook cloud as a bent-back warm front, reminiscent of the term bent back occlusion which is often used to describe it.

(d) Cold conveyor belt constituting a large proportion of the flow within the hook cloud.

Whereas the θ_w = 11°C flow, discussed above, corresponds to air from the warm sector, the θ_w = 10 and 9°C flows in Figs 8(c) and (d) correspond to air that originated just ahead of and beneath the warm front. These flows ascended while travelling generally westward in a system-relative sense within the hook cloud. They correspond to the upper part of Carlson's (1980) cold conveyor belt. At the westernmost limit of these flows, referred to by Carlson (1987) as confluent asymptotes, there is seen to be a marked fanning out of the streamlines, just as there was for the overlying 11°C flow in Fig 8(b), (see also Mass and Schultz 1993). The confluent asymptotes act like material barriers along which airstreams of different origin undergo confluence. Upon reaching the confluent asymptotes (wavy lines in Fig 8) part of each flow turned towards the north and continued ascending; another part turned towards the south, stopped ascending and in some places started to descend. The satellite-detected pattern of the streakiness in the cloud tops associated with the hook cloud (Fig 7(a)) was parallel to these confluent asymptotes. Much of the cold conveyor belt air was ascending and contributing to the growth of precipitation within the hook cloud but, because of the south-north component of the slope of the isentropic surfaces, the ascent decreased or changed into descent in the south-directed portions of these flows. (Later on, when the cyclone began to deepen more rapidly, the southward portions of these diffluent flows strengthened, especially for the lower θ_w-surfaces, and started to carry dissipating low cloud around the southern flank of the cyclone as part of the process of occlusion (Schultz and Mass 1993); however, we shall continue to restrict our attention to the stage just before rapid cyclogenesis and occlusion.)

Comparison of Figs 8 (b), (c) and (d) shows that the air associated with a given confluent asymptote was characterised by a lower θ_w the farther west its confluent asymptote was situated. As each progressively colder θ_w-flow neared its confluent asymptote it emerged from beneath the warmer flows to appear at the top of the hook cloud. The non-overlapping portions of these emerging flows are combined in Fig 8(e) which effectively portrays the flow pattern close to the top of the hook cloud. Comparison of Fig 8(e) with Fig 7(c) confirms that the θ_w-surfaces shown in Fig 8(e) were indeed just beneath the top of the cloud as inferred from the infra-red imagery.

The horizontal extent of significant ascent at 3 km is shown shaded in Fig 9(a), together with an outline of the three flows simplified from Fig 8. Fig 9(a) shows that a zone of frontal ascent extended continuously from the warm front to the hook cloud region behind the part of the cold front corresponding to Shapiro and Keysers' (1990) bent-back warm front. The vertical cross section in Fig 9(b) shows that the strongest ascent above the latter

was due to air with θ_w between 7 and 11°C. Fig 9(c) shows that the strongest ascent above the true warm front was due to air with θ_w between 9 and 13°C. Whereas in the region of a trailing ana-cold front the high-θ_w air in the warm conveyor belt tends to ascend above descending low-θ_w air (Browning and Harrold 1970), in the present case, close to the cyclone centre, both the warm conveyor belt air and the underlying cold conveyor belt air were ascending. Indeed in these regions there was no sharp demarcation between these flows. In this sense the behaviour resembles that described by Kuo et al (1992) (see their Fig 16) who preferred to avoid thinking in terms of discrete conveyor belt flows in such a location. Figs 9(b) and (c) show that, especially in the hook cloud itself, the major proportion of the overall ascent was occurring within cold conveyor belt air. This indicates that, although the warm conveyor belt may be the dominant rain-producing flow for the cyclone overall, including its earlier phase of development, this is not true in the vicinity of the cyclone centre at this stage in the cyclone evolution when the indirect circulation at the exit of jet J_2 converts kinetic energy into potential energy by causing relatively cold air to rise.

(e) Convective precipitation in part of the hook cloud due to the overrunning dry intrusion.

A detailed comparison of the vertical velocity pattern (Fig 9 and other figures not shown) with the observed surface rainfall (Fig 7(b)) shows that moderate to heavy rain fell in the southern part of the hook cloud (over the SW Midlands) where the model-derived large-scale vertical velocities were relatively weak. Fig 7(c) shows that this was a region with low cloud tops that was beginning to be overrun by the dry intrusion. The dry intrusion was introducing slightly lower-θ_w air above saturated 11°C θ_w air corresponding to the W2 flow (Fig 8(b)); the weak large-scale ascent in this region was evidently sufficient to trigger convective precipitation. Although there was only a little thunder over Britain in the present case, this part of a hook cloud is frequently associated with thunder especially in cases with more rapid cyclogenesis. The propensity for convective instability within the W2 warm conveyor belt air is in contrast to the statically stable slantwise ascent that characterizes the cold conveyor belt.

(f) Split front associated with the overrunning dry intrusion in the region of frontal fracture.

The vertical section in Fig 10 passes through the large gap between the two sharp cold frontal segments discussed in Sec. 3b (see X_1X_2 in Fig 7(d)) and it displays characteristics of an incipient 'split cold front' (Browning and Monk 1982). Thus, for example region of cold frontal baroclinicity aloft extends slightly ahead of that at lower levels and there is evidence of the drier air associated with the dry intrusion beginning to overrun moist air in the vicinity of the cold front. A known deficiency of the Unified Model is its overestimation of the relative humidity of upper-level dry zones and we suspect that the model was indeed underestimating the dryness of the dry intrusion in this case. This view is supported by the satellite infrared imagery (Fig 7(a)) and water vapour imagery (not shown) which shows a well defined dry slot penetrating all the way across central England. The right-hand leading edge of the dry intrusion, where it undercuts the high cloud of the polar front cloud band, corresponds to the upper cold front (moisture front) in the split front model, and it produced the area of patchy rain in SE England (Fig 7(b)). This has the appearance of rain generated by weak mid-level convective instability (in this region there was no sign of the line

convection that characterised the sharp surface cold front over Brittany and the Channel). Hence we arrive at the simple analysis scheme (Fig 11) where the upper cold (moisture) front (open frontal symbols) is depicted as a feature distinct from the sharp surface cold front farther south but approximately in line with it at this time. This upper front was not the result of the surface-based cold front riding aloft over the warm sector air but rather, as described by Mass and Schultz (1993), it was due to the dry intrusion causing the downward extension of an upper-level front that extended over only a portion of the lower-tropospheric cold front, in the vicinity of the frontal fracture.

4. Proposed analysis scheme

A simple analysis scheme for a cyclone with hook cloud and frontal fracture is given in Fig 11. The Key to this figure provides a summary of some of the concepts embodied in this paper. The cyclone studied in detail in this paper was a small one. The same processes and structures are thought to occur also in some larger cyclones, but on a larger scale.

The relationship of the proposed analysis scheme to the frontal analysis schemes normally used is shown in Fig 12. Scheme III may be a correct analysis before frontal fracture occurs but there is a tendency for analysts to retain it too long after fracture has begun and then belatedly to jump to Scheme II. An advantage of Scheme I over Scheme II is that it draws a distinction between the region 'ab' where there is a sharp surface front and 'bd' where there is not. A further advantage of Scheme I, is that it draws attention to the effect of the transverse ageostrophic circulation at the exit of an upper level jet in transporting high-θ_w warm-sector air in the boundary layer (from right to left across the jet axis) towards the hook cloud. The same process is believed to generate the frontal fracture described by Shapiro and Keyser (1990).

Acknowledgements

We are grateful to M J Bader, Dr S A Clough, R Grant and M V Young for their helpful comments on an earlier draft.

References

Bader, M.J., Forbes, G.S., Grant, J.R., Lilley, R.B.E. and Waters, A.J. (Eds)	1993	Images in weather forecasting. Cambridge University Press. In press.
Bottger, H., Eckardt, M. and Katergiannakis, U.	1975	Forecasting extratropical storms with hurricane intensity using satellite information. J.Appl.Meteorol., **14**, 1259-1265.
Browning, K.A. and Harrold, T.W.	1970	Air motion and precipitation growth at a cold front. Q.J.R.Meteorol.Soc., **96**, 369-389.
Browning, K.A. and Monk, G.A.	1982	A simple model for the synoptic analysis of cold fronts. Q.J.R.Meteorol.Soc., **108**, 435-452.
Carlson, T.N.	1980	Airflow through midlatitude cyclones and the comma cloud pattern. Mon.Wea.Rev., **108**, 1498-1509.
Carlson, T.N.	1987	Cloud configuration in relation to relative isentropic motion. Satellite and radar imagery interpretation (preprint vol., workshop at UK Meteorol.Office), Eds. M.Bader and T.Waters. EUMETSAT, Darmstadt, FRG, 43-61.
Harrold, T.W.	1973	Mechanisms influencing the distribution of precipitation within baroclinic disturbances. Q.J.R.Meteorol.Soc., **99**, 232-251.
Hobbs, P.V. and Biswas, K.R.	1979	The cellular structure of narrow cold-frontal rainbands. Q.J.R.Meteorol.Soc., **105**, 723-727.
Hoskins, B.J., McIntyre, M.E. and Robertson, A.W.	1985	On the use and significance of isentropic potential vorticity maps. Q.J.R.Meteorol.Soc., **111**, 877-946.
James, P.K. and Browning, K.A.	1979	Mesoscale structure of line convection at surface cold fronts. Q.J.R.Meteorol.Soc., **105**, 371-382.
Kuo, Y.-H., Reed, R.J. and Low-Nam, S.	1992	Thermal structure and airflow in a model simulation of an occluded maritime cyclone. Mon.Wea.Rev., **120**, 2280-2297.
Mass, C.F. and Schultz, D.M.	1993	The structure and evolution of a simulated midlatitude cyclone over land. Mon.Wea.Rev., **121**, 889-917.
McBean, G.A. and Stewart, R.E.	1991	Structure of a frontal system over the northeast Pacific Ocean. Mon.Wea.Rev., **119**, 997-1013.
McCallum, E. and Norris, W.J.T.	1990	The storms of January and February 1990. Meteorol.Mag., **119**, 201-210.
McGinnigle, J.B., Young, M.V. and Bader, M.J.	1988	The development of instant occlusions in the north Atlantic. Meteorol.Mag., **117**, 325-341.
Neiman, P.J., Shapiro, M.A. and Fedor, L.S.	1993	The life cycle of an extratropical marine cyclone. Part II: Mesoscale structure and diagnostics. Submitted to Mon.Wea.Rev.

Newton, C.W. and Holopainen, E.O. (eds)	1990	Extratropical cyclones, The Erik Palmén Memorial Volume, Amer.Meteorol.Soc., Boston, Mass., 262 pp.
Reed, R.J. and Danielsen, E.F.	1959	Fronts in the vicinity of the tropopause. Arch.Meteor.Geophys.Bioklim., **A11**, 1-17.
Sanders, F. and Gyakum, J.R.	1980	Synoptic-dynamic climatology of the "bomb". Mon.Wea.Rev., **108**, 1589-1606.
Schultz, D.M. and Mass, C.F.	1993	The occlusion process in a midlatitude cyclone over land. Mon.Wea.Rev., **121**, 918-940.
Shapiro, M.A. and Keyser, D.	1990	Fronts, jet streams and the tropopause. In Extratropical cyclones. Eds. Newton, C.W. and Holopainen, E.O. Amer.Meteorol.Soc., Boston, Mass., 167-191.
Shutts, G.J.	1990	Dynamical aspects of the October storm, 1987: a study of a successful fine-mesh simulation. Q.J.R.Meteorol.Soc., **116**, 1315-1347.
Thorpe, A.J. and Emanuel, K.A.	1985	Frontogenesis in the presence of small stability to slantwise convection, J.Atmos.Sci., **42**, 1809-1824.
Uccellini, L.W.	1990	Processes contributing to the rapid development of extratropical cyclones. In Extratropical cyclones. Eds. Newton, C.W. and Holopainen, E.O.., Amer.Meteorol.Soc., Boston, Mass., 81-105.
Uccellini, L.W. and Johnson, D.R.	1979	The coupling of upper and lower tropospheric jet streaks and implications for the development of severe convective storms. Mon.Wea.Rev., **107**, 682-703.
Weldon, R.B.	1979	Satellite training course notes. Part IV. Cloud patterns and upper air wind field. United States Air Force, AWS/TR-79/003.
Weldon, R.B. and Holmes, S.J.	1991	Water vapor imagery: interpretation and applications to weather analysis and forecasting. NOAA Tech.Rep. NESDIS 57. US Dept. of Commerce, Washington DC. 213pp.
Young, M.V.	1989	Investigation of a cyclogenesis event, 26-29 July 1988, using satellite imagery and numerical model diagnostics. Meteorol.Mag., **118**, 185-196.
Young, M.V., Monk, G.A. and Browning, K.A.	1987	Interpretation of satellite imagery of a rapidly deepening cyclone. Q.J.R.Meteorol.Soc., **113**, 1089-1115.

Figure Legends

Fig 1 — 300 mb analyses for 12 UTC, 12 January 1993. Height contours in dam. Light, medium and dark stipple represent 300 mb windspeeds in excess of 25, 30 and 35 ms^{-1}, respectively. The position of the cyclone of interest is labelled X.

Fig 2 — Surface analyses superimposed on METEOSAT infra-red imagery (cold high cloud, white) for (a) 12 UTC, 12 January and (b) 15 UTC, 13 January 1993. The cyclone of interest is labelled LOW X. Coastlines, omitted from (b) to avoid obscuring the cloud features, are situated exactly as in (a).

Fig 3 — METEOSAT infra-red imagery for parts of the area in Fig 2 showing the evolution of the hook cloud at mainly 6-h intervals from 09 UTC 12 January to 21 UTC, 13 January 1993. The projection is the same as in Fig 2, each frame being displaced by an equal distance towards the right to keep the developing cyclone within the field of view. X marks the location of the cyclone. The hook cloud is first seen at 13/03Z, 7 degrees west of X; by 13/21Z the edge of the hook cloud has become coincident with X.

Fig 4 — Sequence of 3-h model forecasts for times indicated, showing 300 mb windspeed derived from the model. X marks the cyclone centre.

Fig 5 — Sequences as in Fig 3 but for the following low-level model products: (a) θ_w and windspeed at 900 mb and (b) potential vorticity at 900 mb. The unit of PV is 10^{-6} m^2 s^{-1} K kg^{-1}. X marks the cyclone centre.

Fig 6 — Sequence as in Fig 3 but for the height of the PV=2 surface, corresponding to the dynamical tropopause. X marks the cyclone centre.

[PRINTER: please reproduce Figures 3, 4, 5 and 6 all to same scale for easy intercomparison].

Fig 7 (a and b) Imagery of the cyclone at about 15 UTC, 13 January 1993. (a) METEOSAT infra-red imagery at 15 UTC, showing the hook cloud extending from eastern Ireland and St George's Channel, across northern England and southern Scotland, into the North Sea, and (b) the weather radar picture at 1530 UTC. Colour codes give (a) brightness temperature in °C and (b) estimated rainfall intensity in mm h^{-1}. The projection in (a) (as in c, d and e) is polar stereographic, whereas that in (b) is transverse Mercator.

Fig 7(c) Cloud tops and surface rainfall pattern for 15 UTC, 13 January 1993 derived from the imagery in Fig 7 (a and b). Isopleths of cloud height are at 3, 6 and 8 km. Areas of rain are stippled. Also shown is the model-derived dry intrusion (broad arrow gives its extent in the 30°C θ-surface, which was located at a height of between 5 and 7 km).

Fig 7(d) Model-derived surface pressure (solid curve at 4 mb intervals) and 900 mb θ_w (dotted curves at 1°C intervals) for 15 UTC, 13 January 1993. Arrows show ageostrophic flow at 900 mb. The observed positions of sharp surface fronts are also shown. The dashed curve is explained in the text. X_1X_2 shows the location of the vertical section in Fig 10.

Fig 7(e) Observed surface wet bulb potential temperature for 15UTC, 13 January 1993. Individual station values of wet bulb temperature, adjusted to 1000 mb according to available tephigrams, are plotted to the nearest ½°C (½ is indicated by •) and the corresponding isopleths are drawn at 1°C intervals.

Fig 8 Model-derived moist isentropic flow relative to the cyclone at 15 UTC, 13 January 1993. The cyclone was travelling with a component of 23.5 m s^{-1} toward the top and 18.8 m s^{-1} toward the right of the diagram. The selected θ_w-surfaces correspond to those in the lower part of the warm conveyor belt (θ_w = 12 and 11°C) and the upper part of the cold conveyor belt (θ_w = 10 and 9°C).

(a) Direct model output for flow in the θ_w = 11°C surface. Arrows represent relative flow and shading represents height at 2 km intervals, dark areas corresponding to 0-2 km (SE corner), 4-6 km and 8-10 km.

(b) Relative flow in the θ_w = 11°C surface (solid curves) and height of that surface at 1 km intervals (dashed curves), derived from (a).

(c) & (d) Same as (b) but for relative flow in the θ_w = 10°C and 9°C surfaces, respectively.

(e) Superposition of flow pattern from (b), (c) and (d) where the flows emerge at the top of the hook cloud, plus the relative flow in the cloudy part of the θ_w = 12°C surface.

Fig 9(a) Model-derived pattern of 700 mb vertical velocity at 15 UTC, 13 January 1993 (light stipple >2 cm s^{-1}, medium stipple >6 cm s^{-1}) superimposed on relative flows in the θ_w = 12°C surface (broad arrow), 11°C surface (arrow entering from east and turning north) and 10°C and 9°C surfaces (arrows entering from east and then fanning out to the north and south). B_1B_2 and C_1C_2 show the locations of the vertical sections in Figs 9(b) and (c).

Fig 9 (b and c) Model-derived flow relative to the cyclone in the vertical sections along B_1B_2 and, C_1C_2 in Fig 9(a). Arrows denote relative flow and the dark shading denotes relative humidity exceeding 95%. Black isopleths and white isopleths, respectively, denote θ_w at 2°C intervals and vertical velocity for 4 and 8 cm s^{-1}.

Fig 10 Model-derived cross-section along X_1X_2 in Fig 7(d) showing the dry intrusion beginning to overrun the moist zone of high-θ_w air. Solid lines denote θ_w at 1°C intervals, dashed lines denote potential temperature, θ, at 10°C intervals and shading denotes relative humidity (grey >90%, light grey >70%, very light grey >30%, white ≤30%). The locations of the dry intrusion (broad arrow) and of the diffuse surface cold front (SCF) and upper cold front (UCF) are also indicated. Note the weak potential instability in the lower portion of the dry intrusion.

Fig 11 Simple analysis scheme for a cyclone with hook cloud and frontal fracture, prior to occlusion. See key. The details of this analysis are based on observational data for the present case study at 15UTC, 13 January 1993.

Fig 12 Relationship of the proposed analysis scheme (I) to the kind of analyses normally used (II or III). The letters denote corresponding locations in the different analyses.

Fig 1

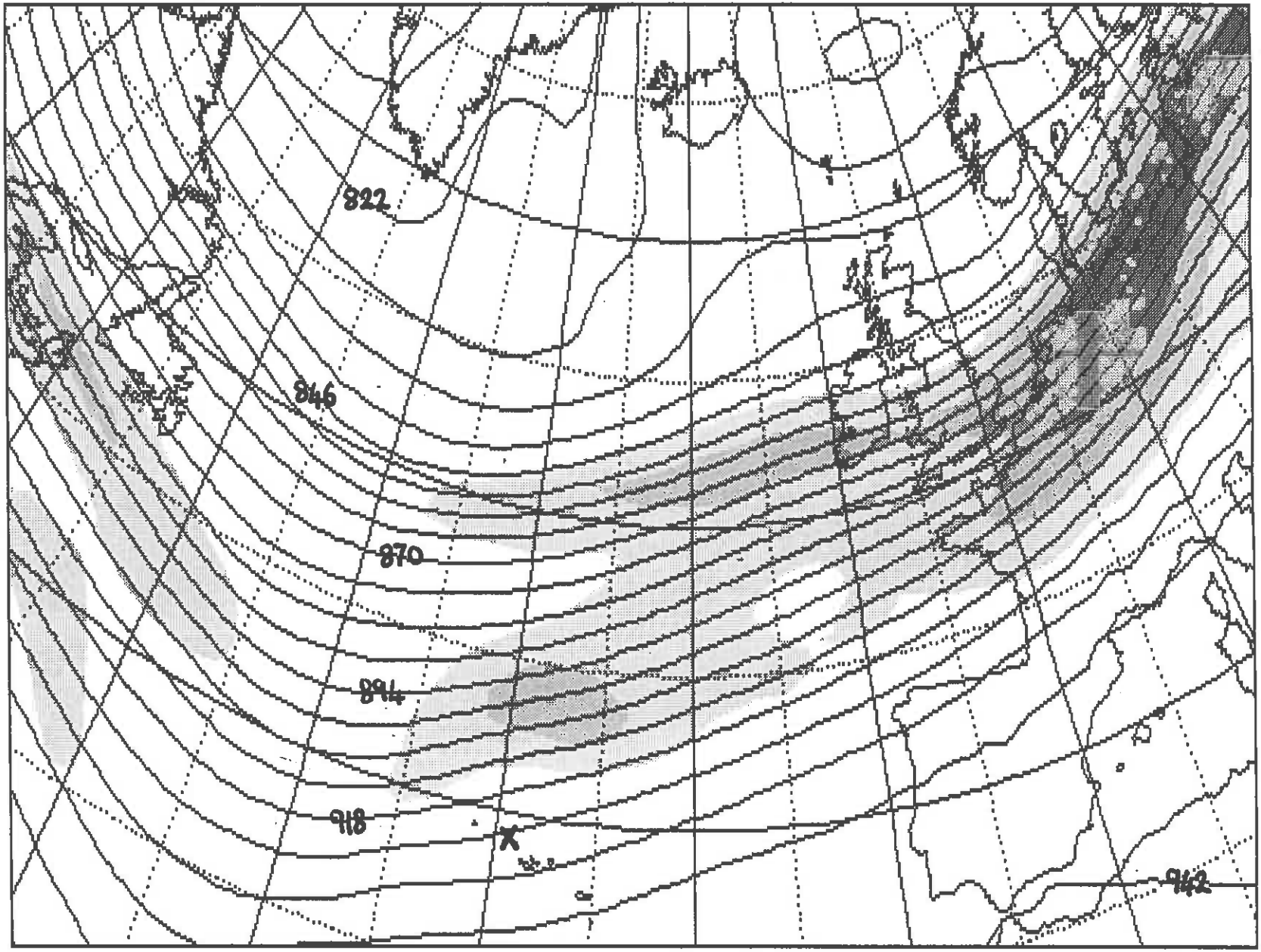

Fig 2a

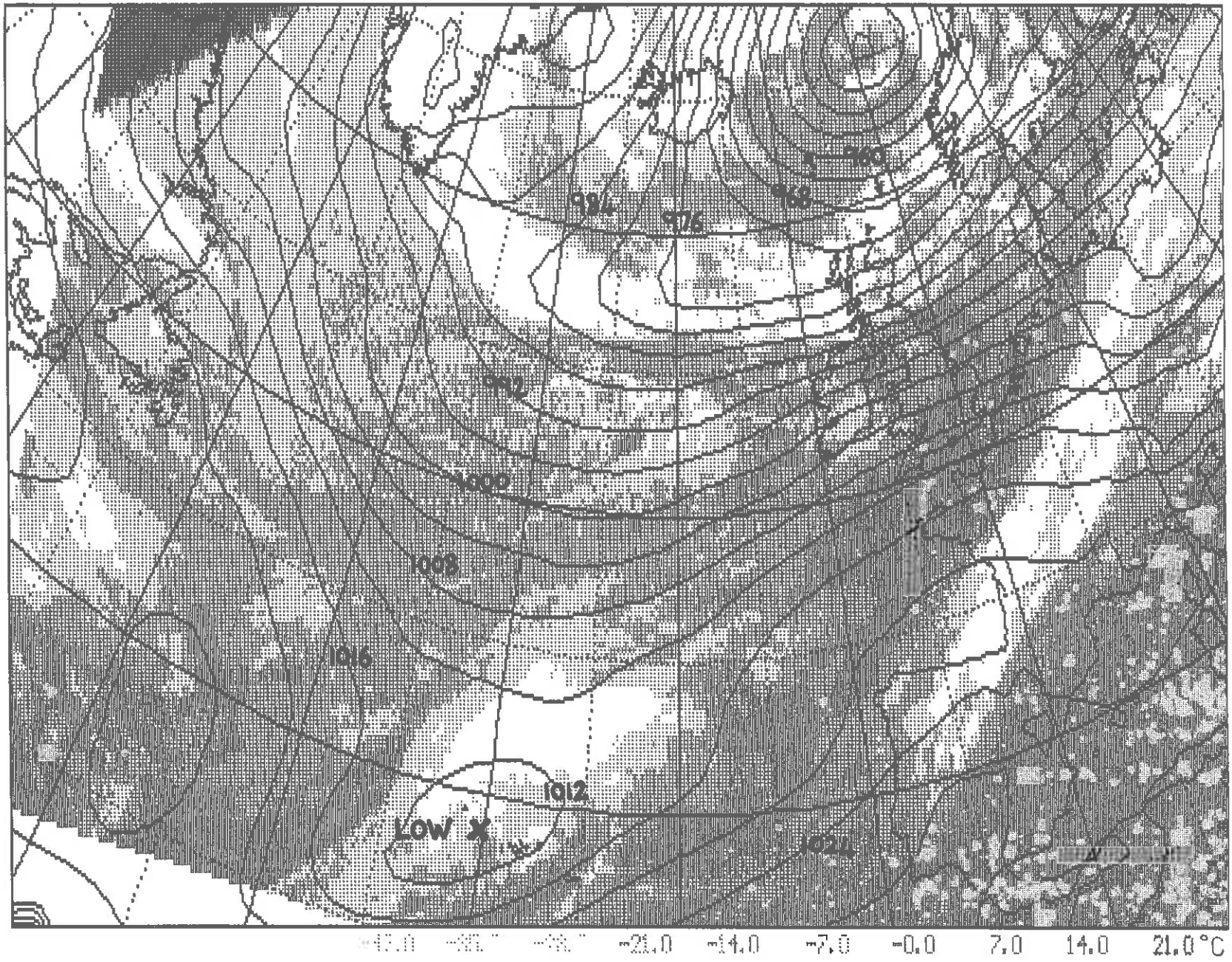
994
996
998
1000
1004
1008
1016
1012
Low X
1024
-21.0
-14.0
-7.0
-0.0
7.0
14.0
21.0 °C

Fig 2b

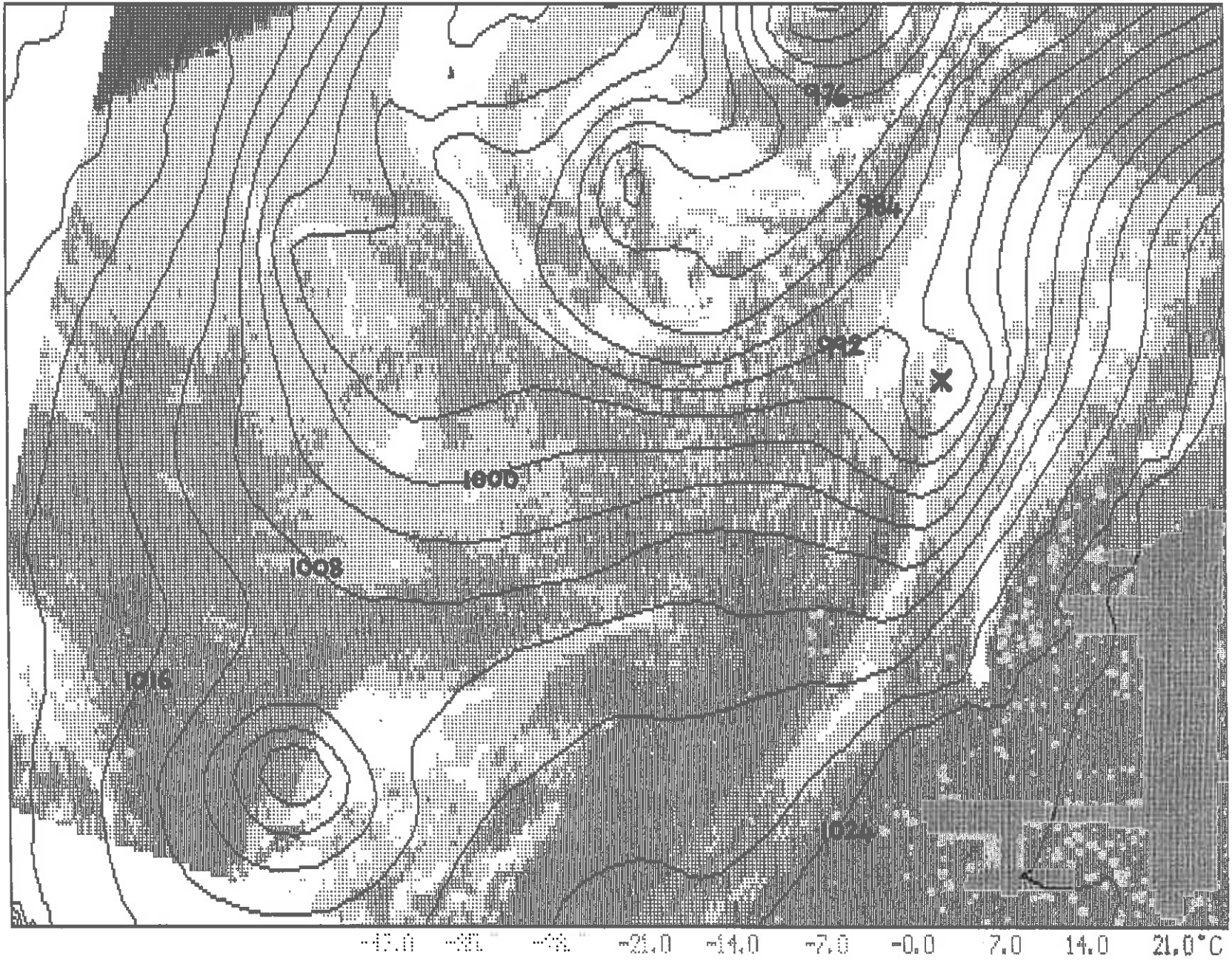

Fig 3

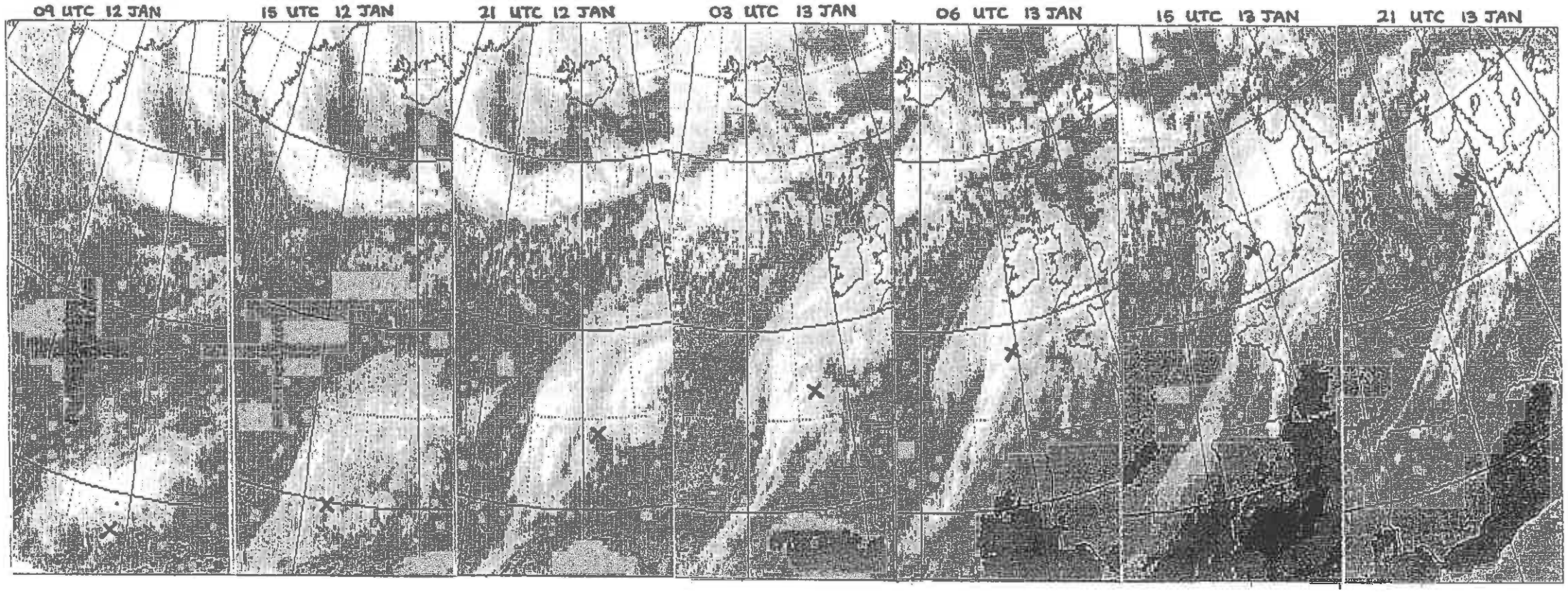
09 UTC 12 JAN
15 UTC 12 JAN
21 UTC 12 JAN
03 UTC 13 JAN
06 UTC 13 JAN
15 UTC 13 JAN
21 UTC 13 JAN

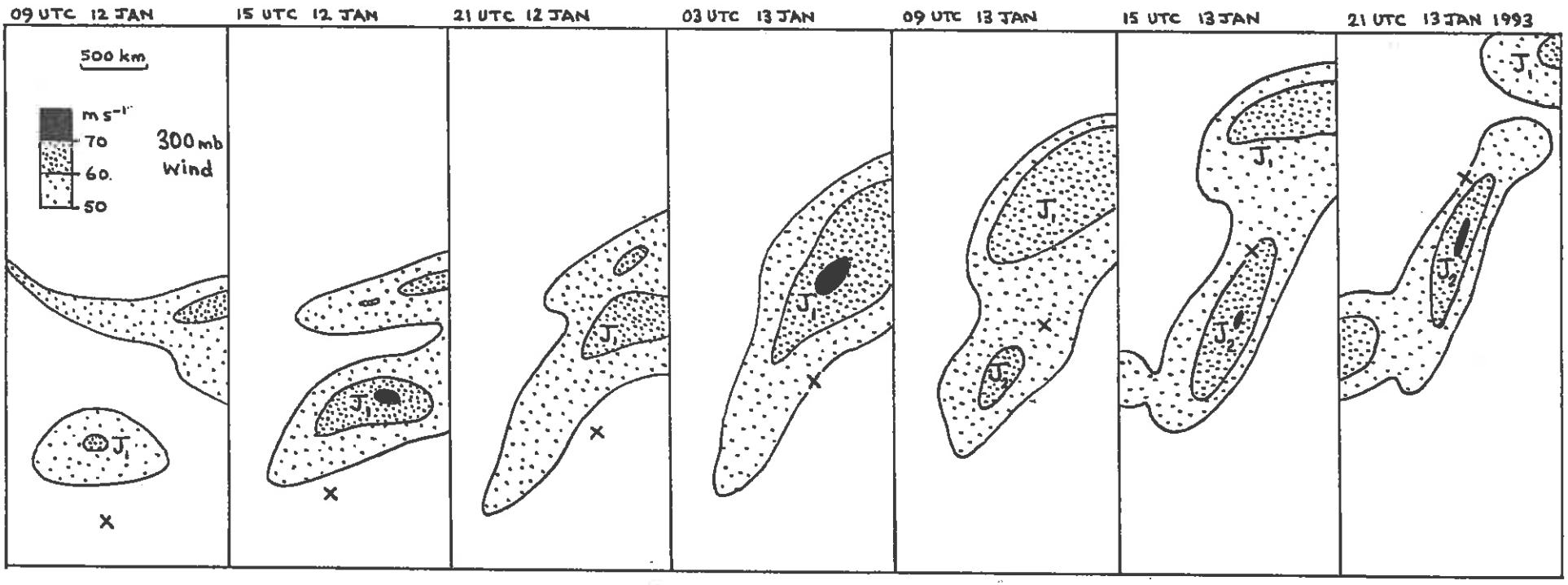
09 UTC 12 JAN
15 UTC 12 JAN
21 UTC 12 JAN
03 UTC 13 JAN
09 UTC 13 JAN
15 UTC 13 JAN
21 UTC 13 JAN 1993
500 km
m s⁻¹
70
60
50
300 mb
Wind
J1
J2
X

Fig 4

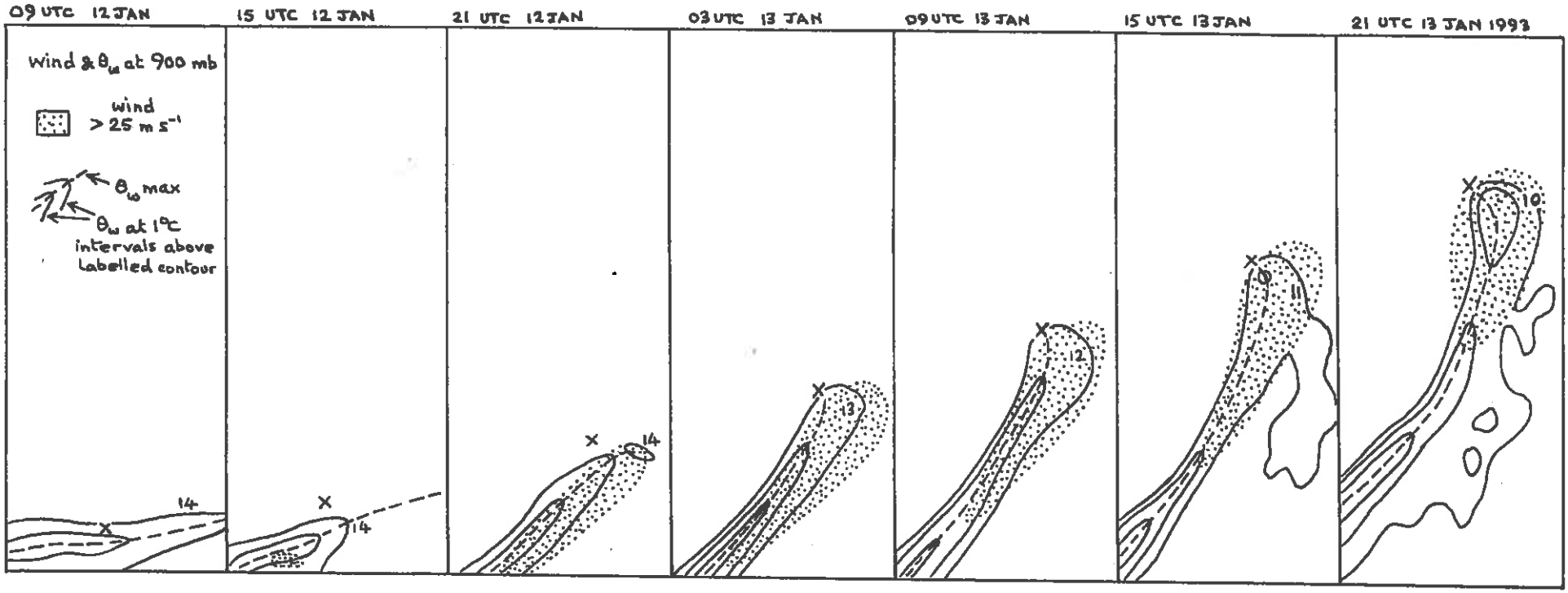
09 UTC 12 JAN
15 UTC 12 JAN
21 UTC 12 JAN
03 UTC 13 JAN
09 UTC 13 JAN
15 UTC 13 JAN
21 UTC 13 JAN 1993
Wind & θ_w at 900 mb
wind
> 25 m s^{-1}
θ_w max
θ_w at 1°C
intervals above
labelled contour
14
14
14
13
12
11
10

Fig 5(a)

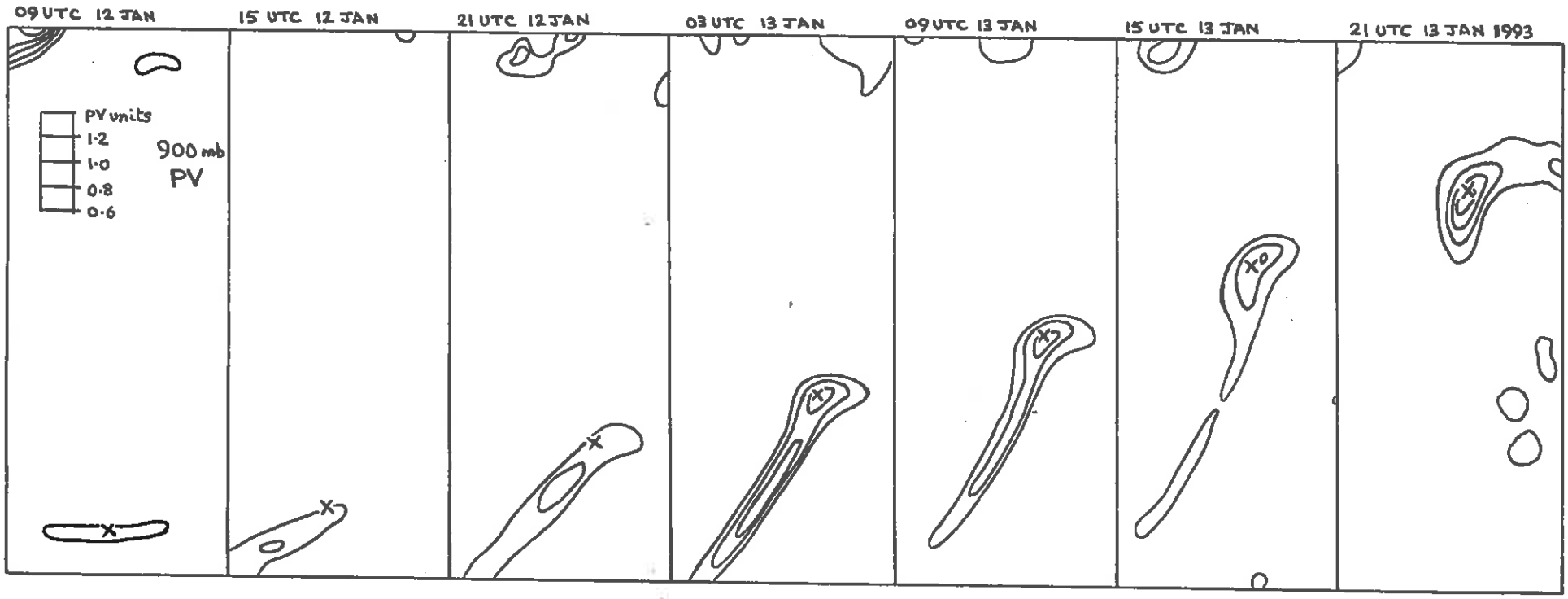
09 UTC 12 JAN
15 UTC 12 JAN
21 UTC 12 JAN
03 UTC 13 JAN
09 UTC 13 JAN
15 UTC 13 JAN
21 UTC 13 JAN 1993
PV units
1·2
1·0
0·8
0·6
900 mb
PV

Fig 5(b)

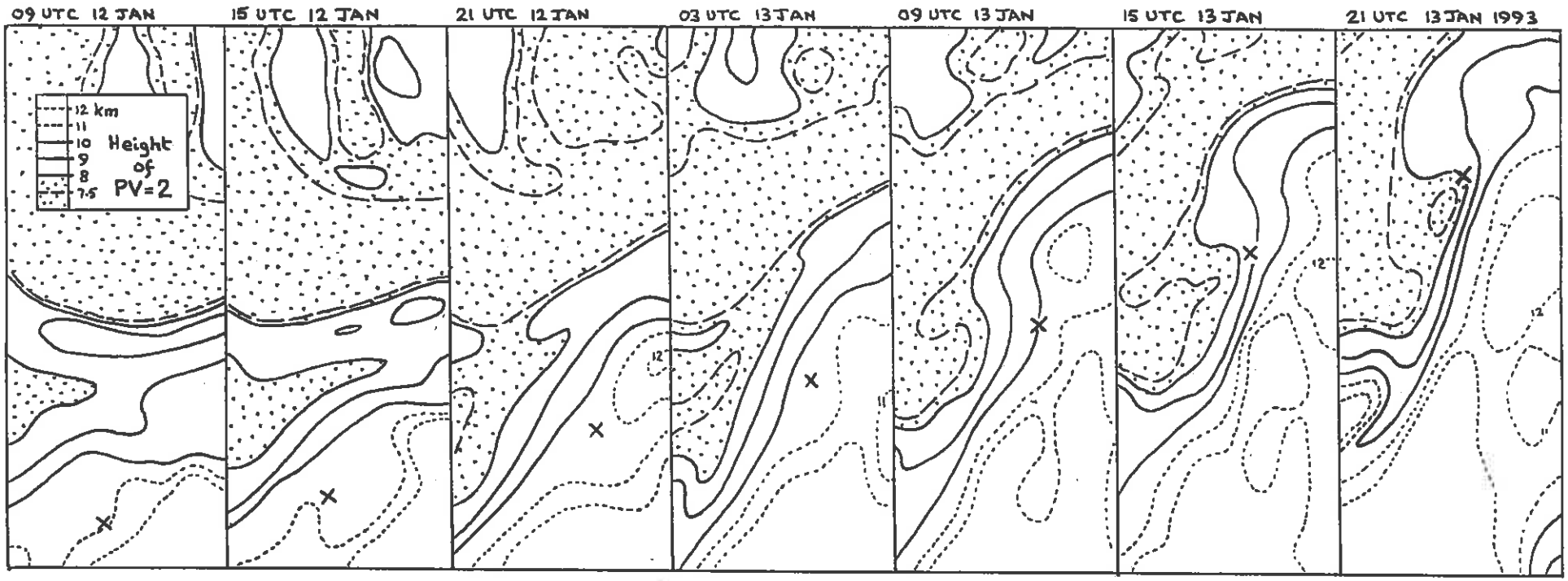
09 UTC 12 JAN
15 UTC 12 JAN
21 UTC 12 JAN
03 UTC 13 JAN
09 UTC 13 JAN
15 UTC 13 JAN
21 UTC 13 JAN 1993
12 km
11
10
9
8
7.5
Height of PV=2

Fig 6

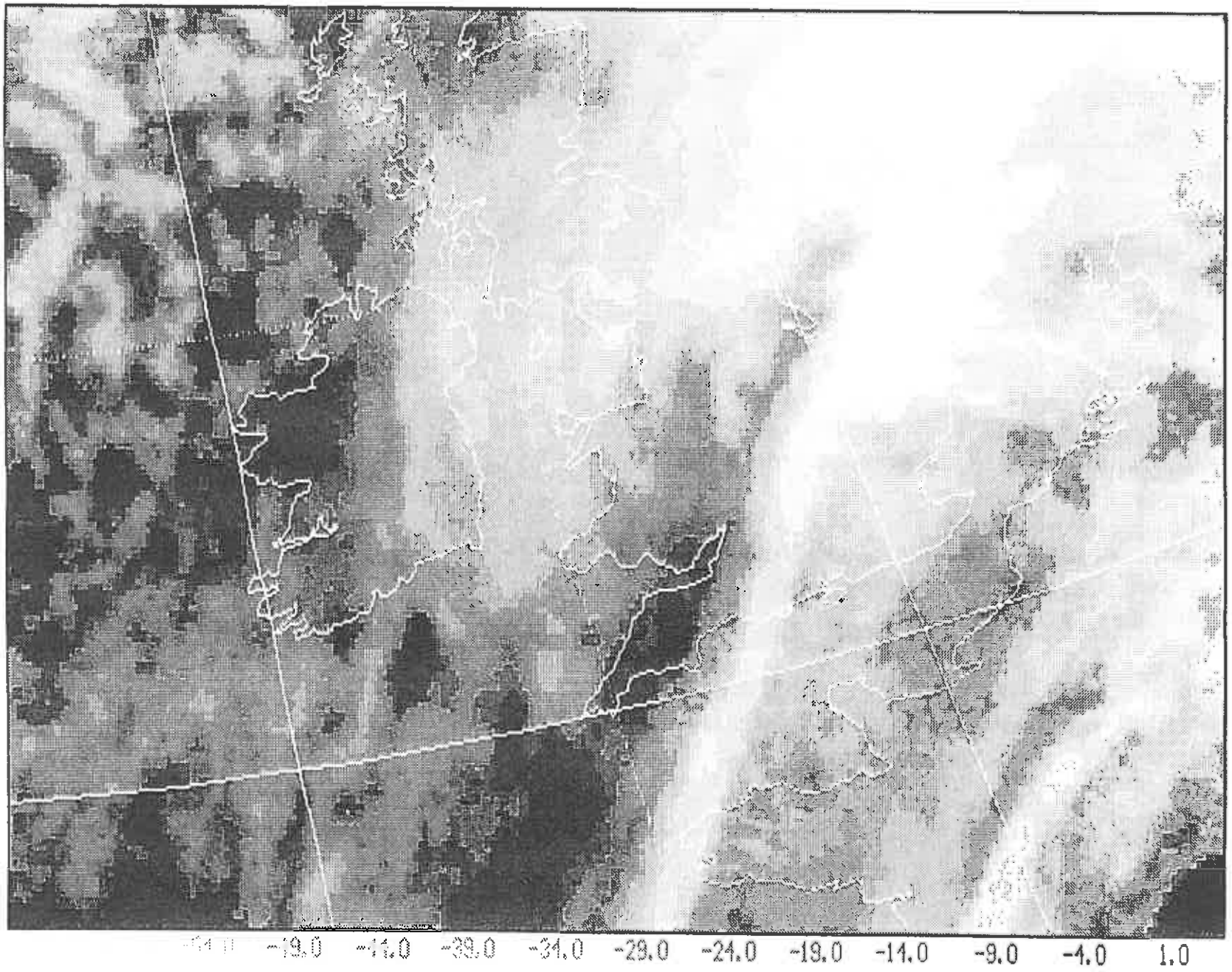

Fig 7(a)

Fig 7(b)

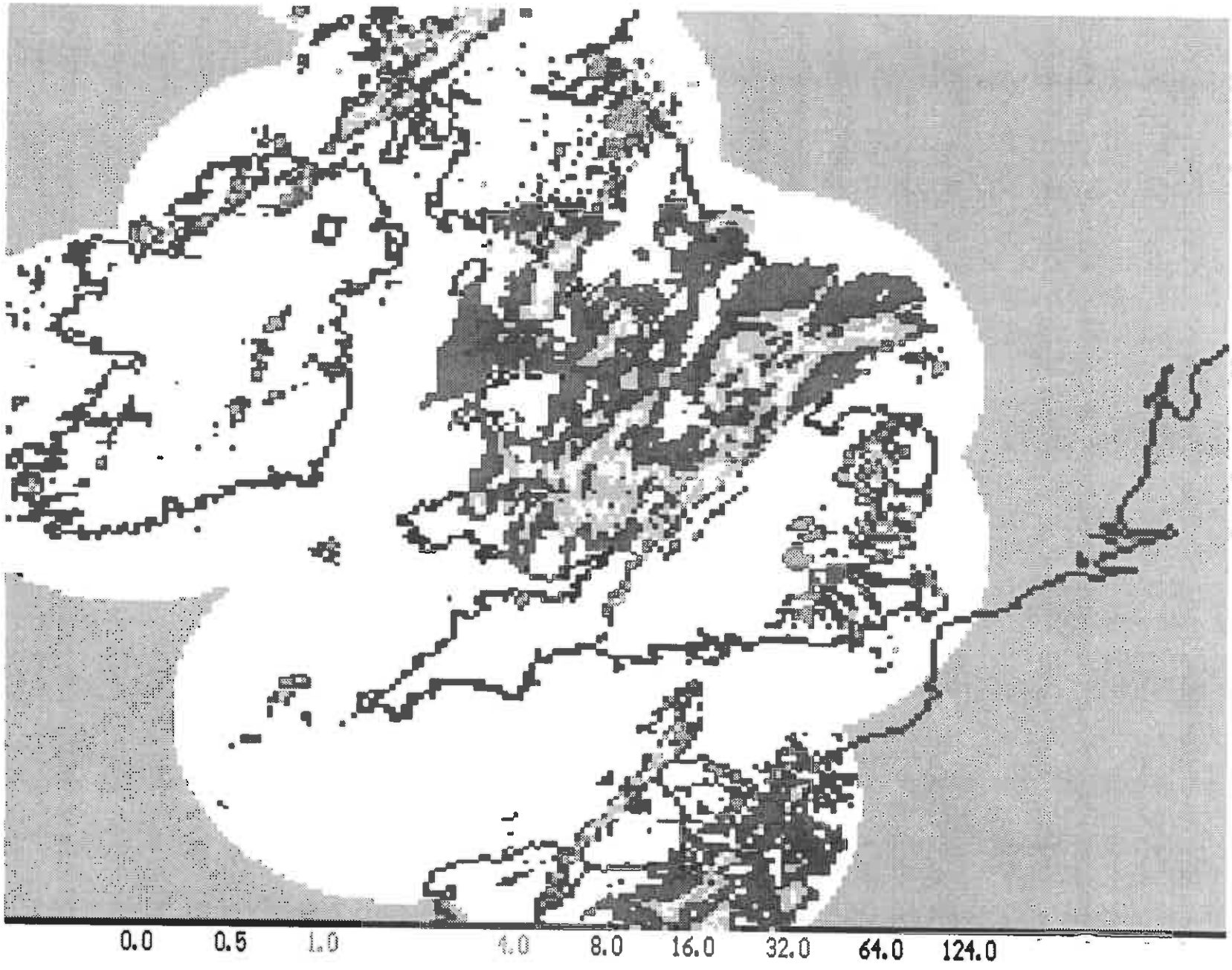

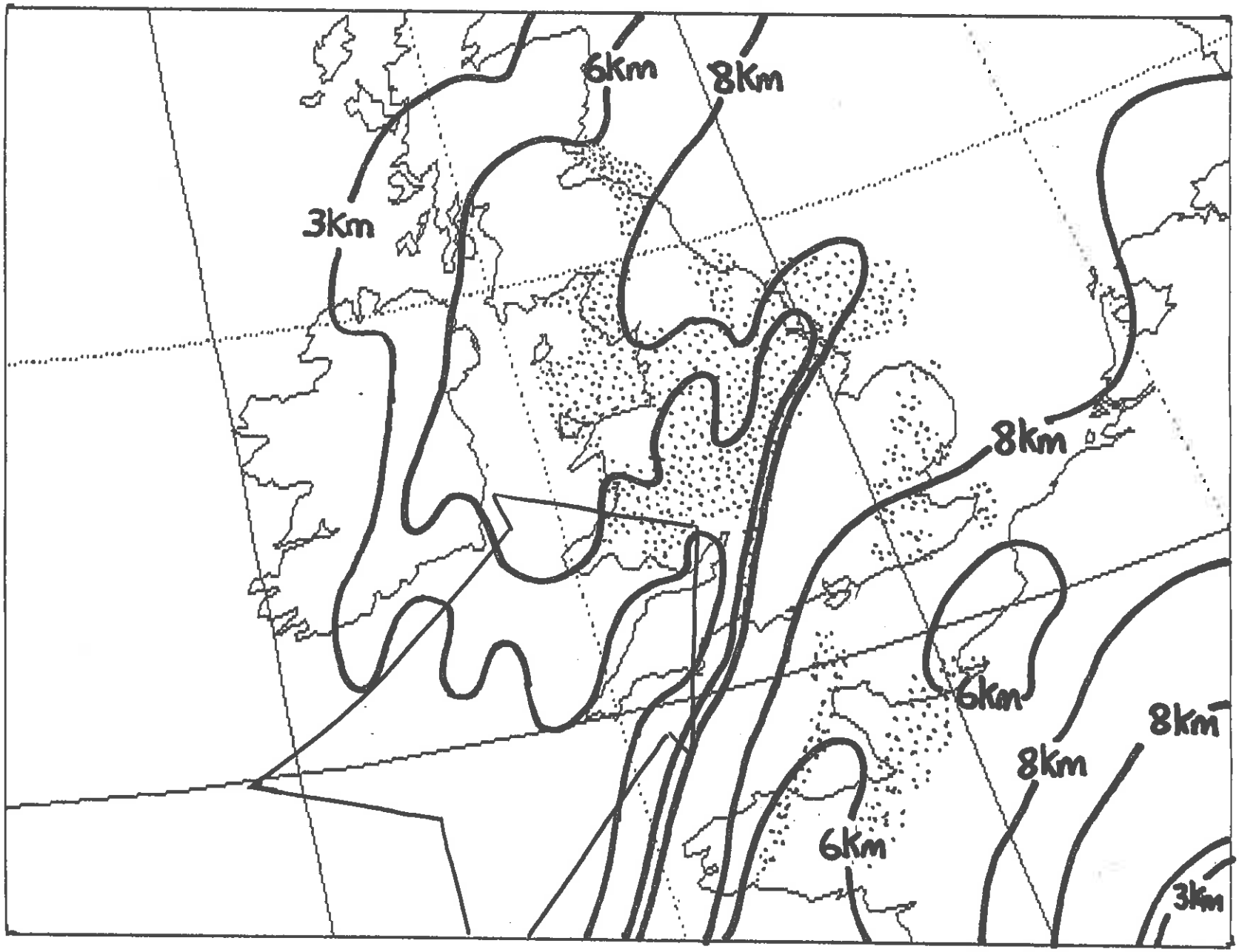

Fig 7(c)

Fig 7d

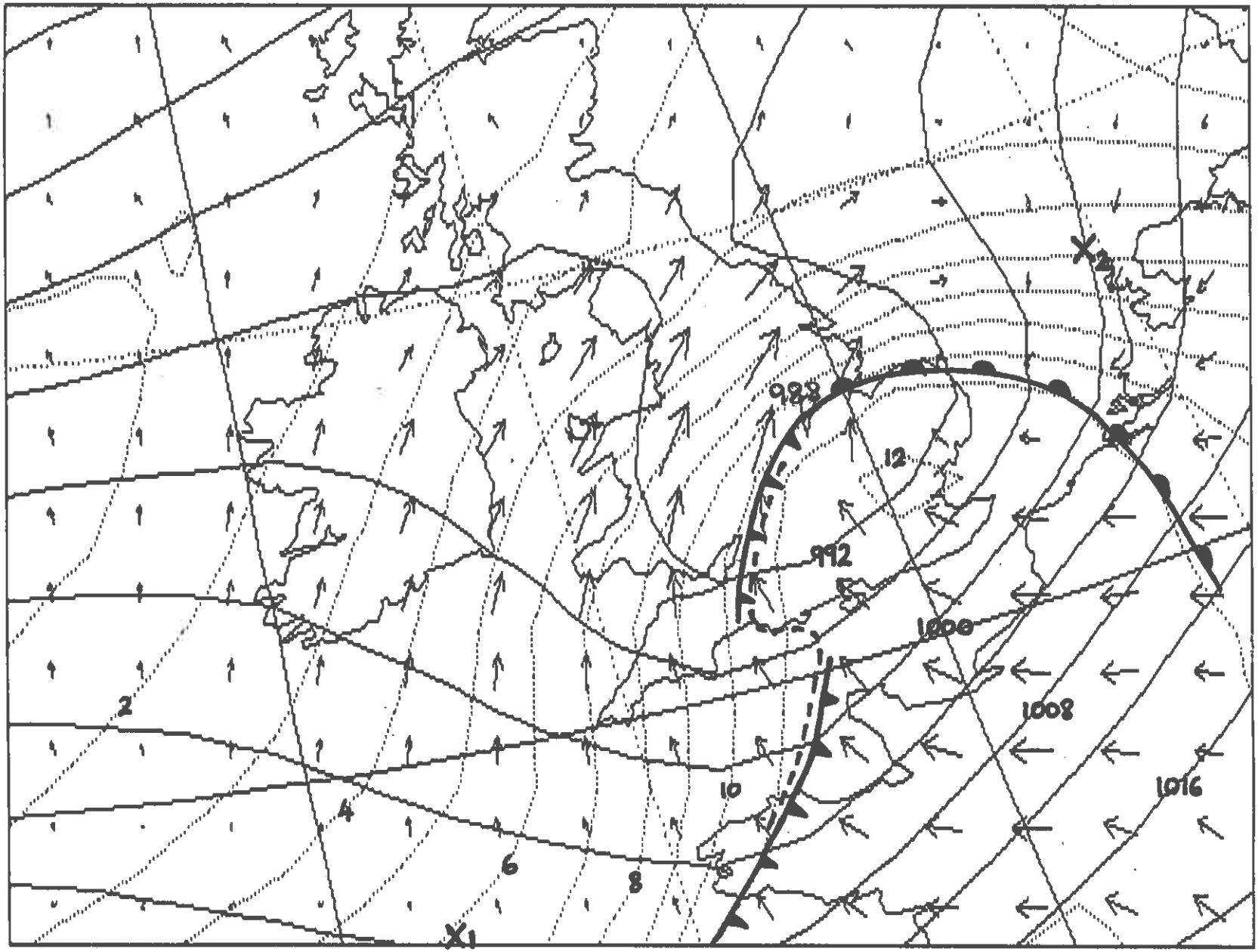

→ = 4.0 m/s ↑ = 4.0 m/s

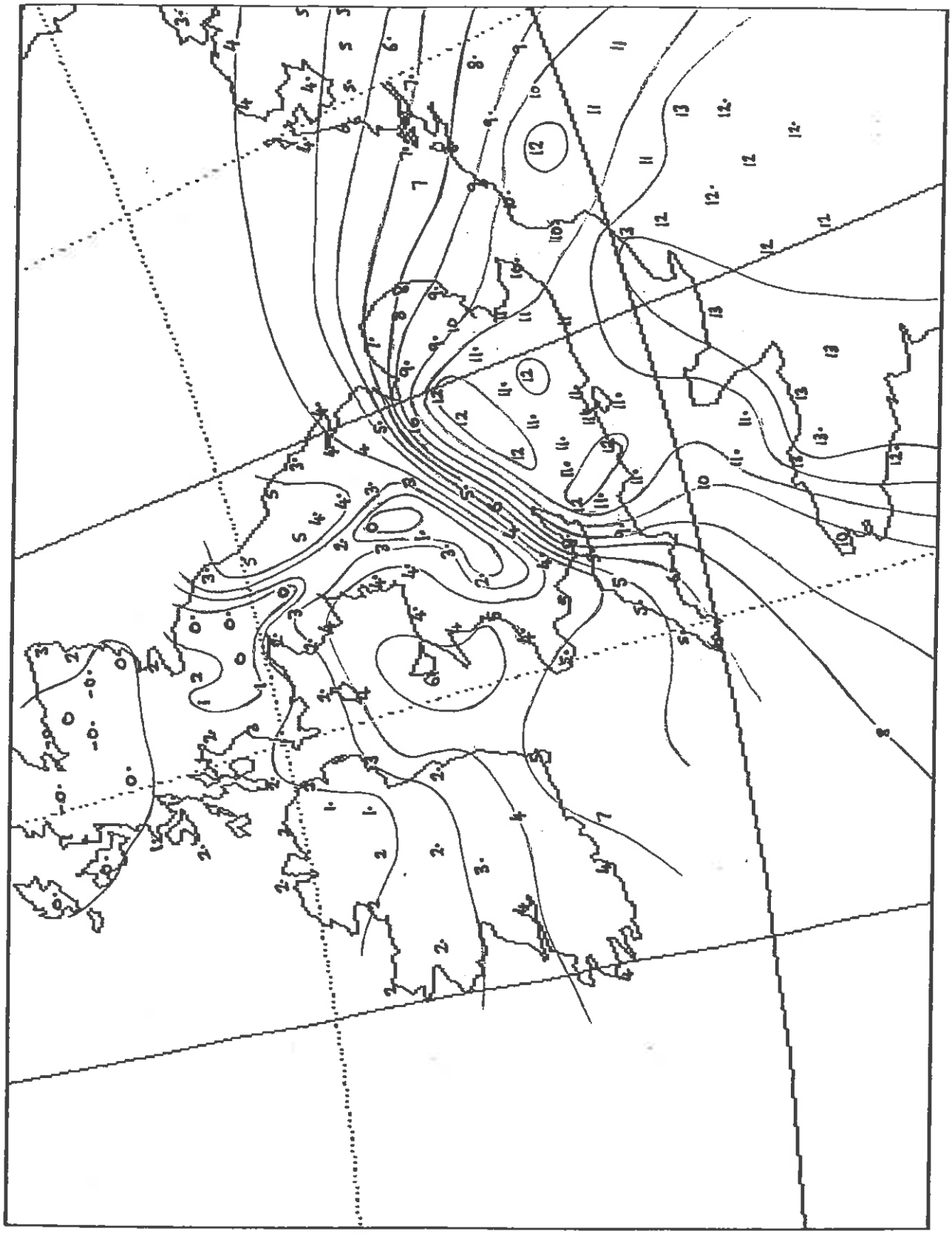

Fig. 7e

Fig 8a

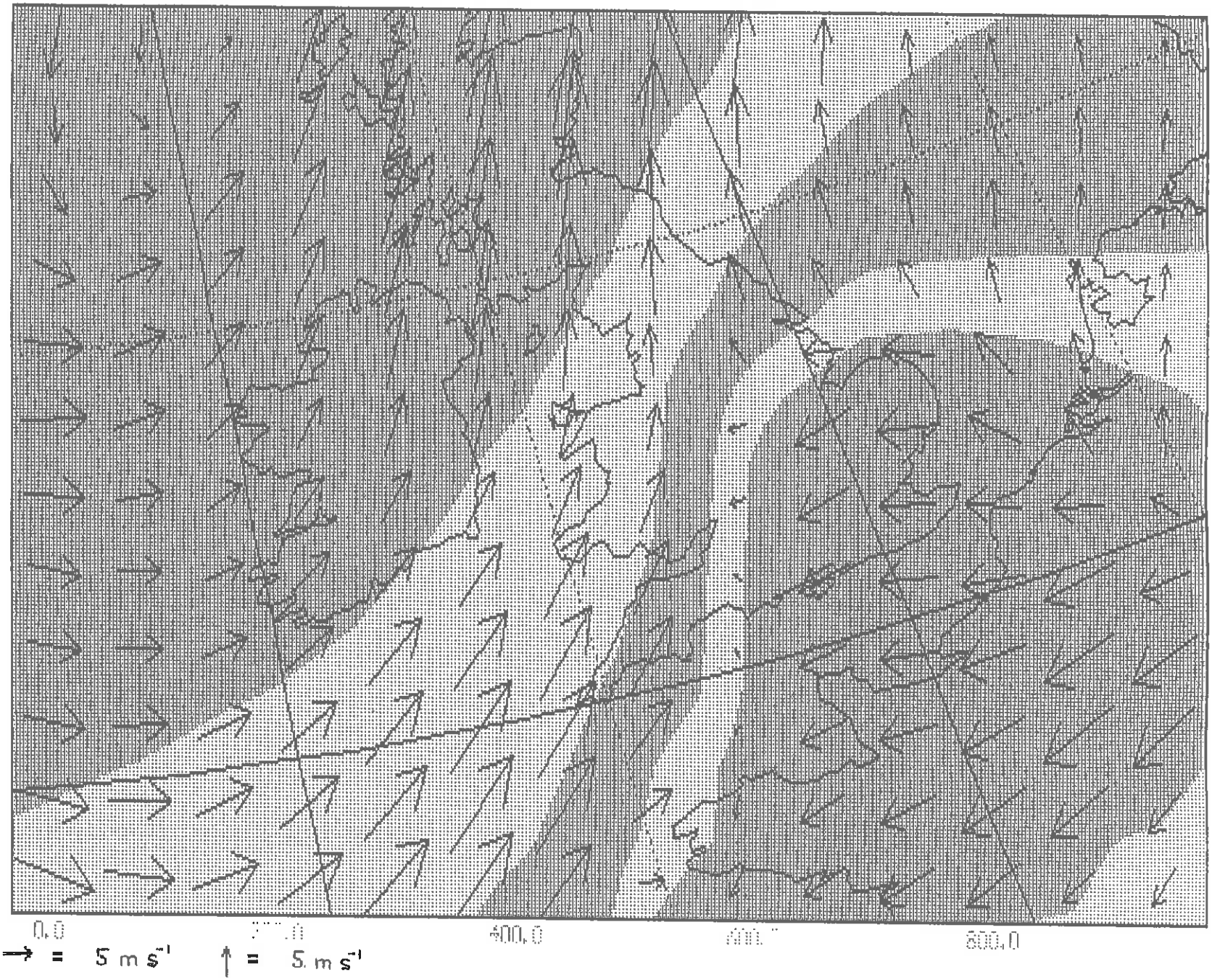

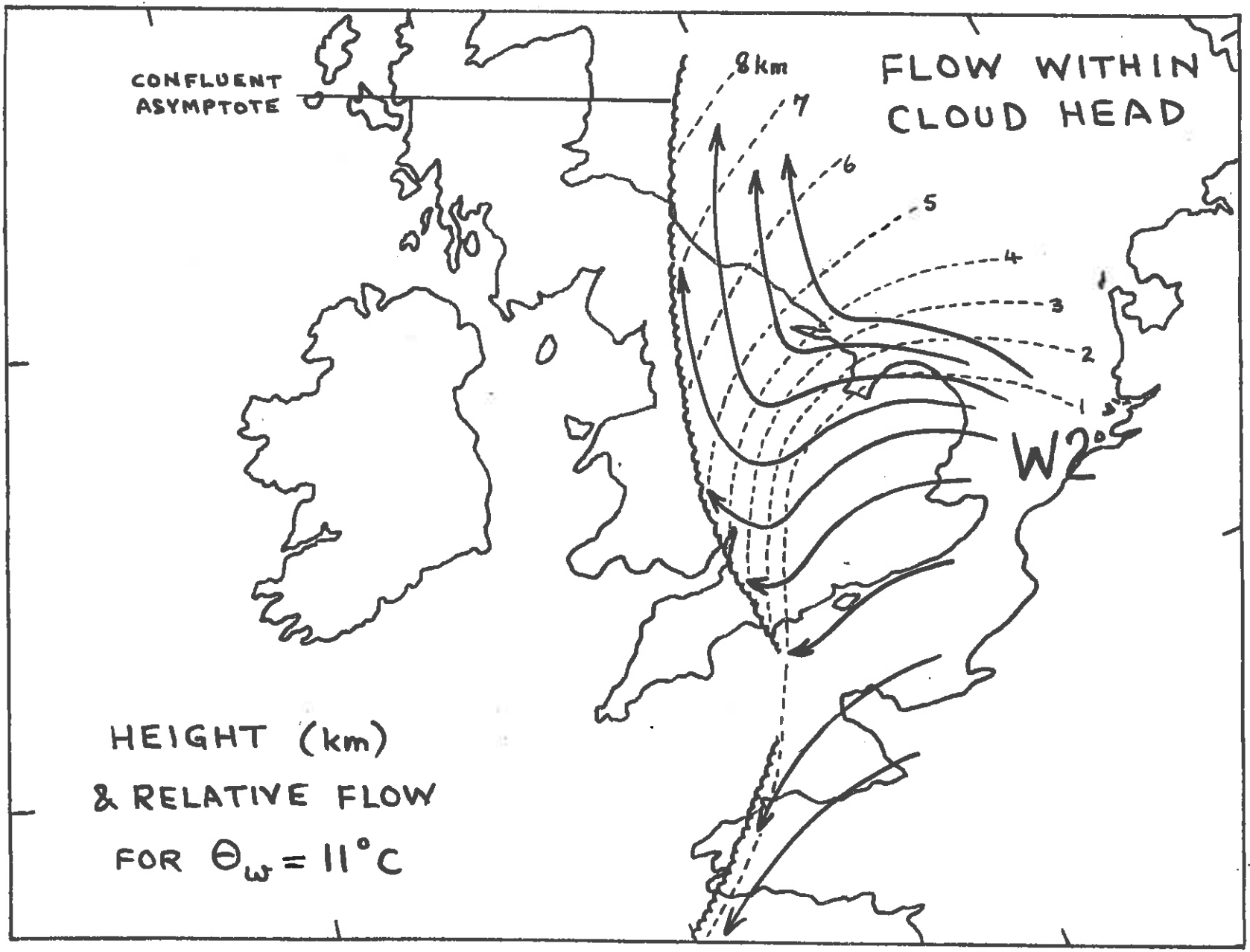
CONFLUENT
ASYMPTOTE
8km
7
6
5
4
3
2
1
FLOW WITHIN
CLOUD HEAD
W2°
HEIGHT (km)
& RELATIVE FLOW
FOR $\Theta_w = 11°C$

Fig 8(b)

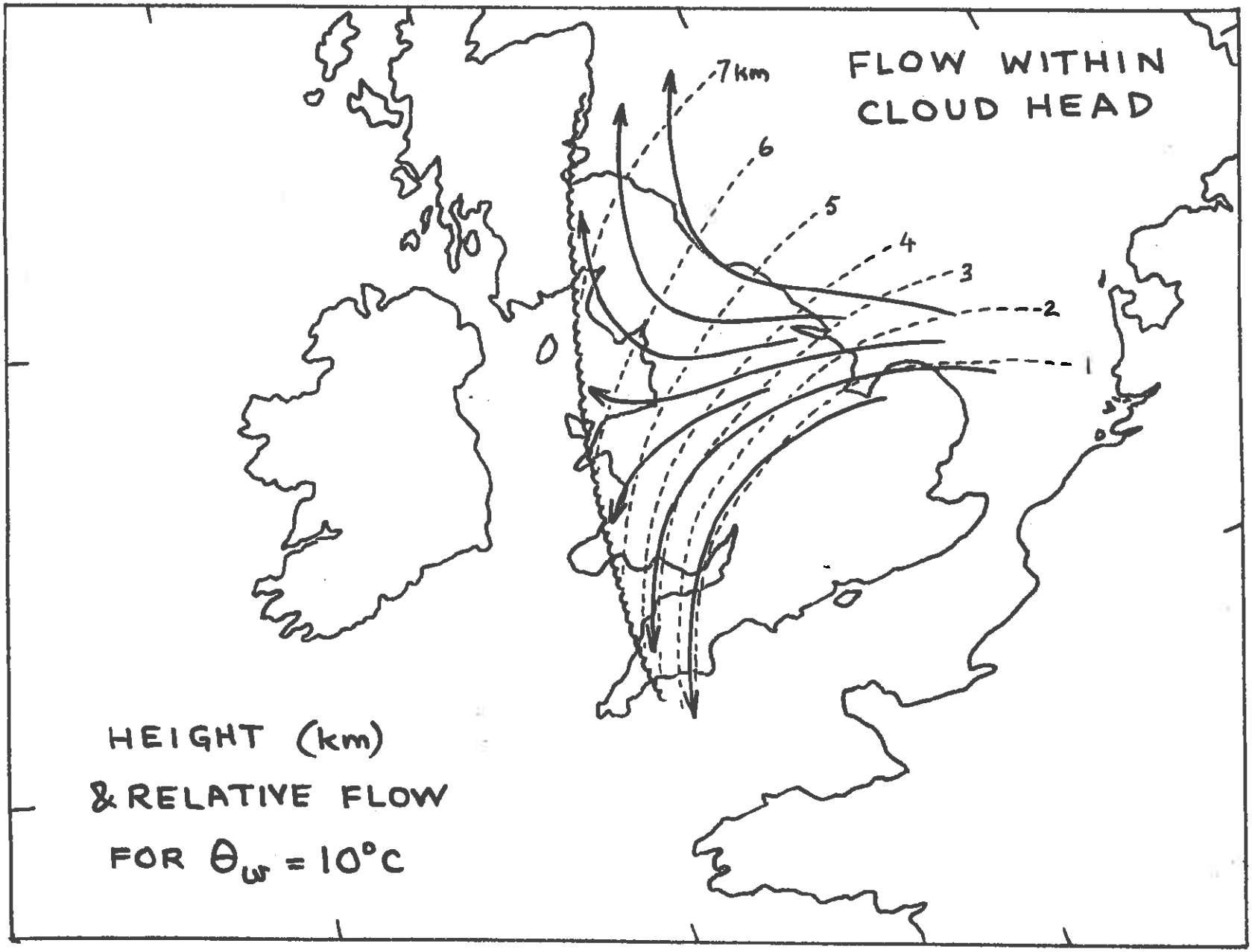
FLOW WITHIN
CLOUD HEAD
7km
6
5
4
3
2
1
HEIGHT (km)
& RELATIVE FLOW
FOR θ_w = 10°C

Fig 8(c)

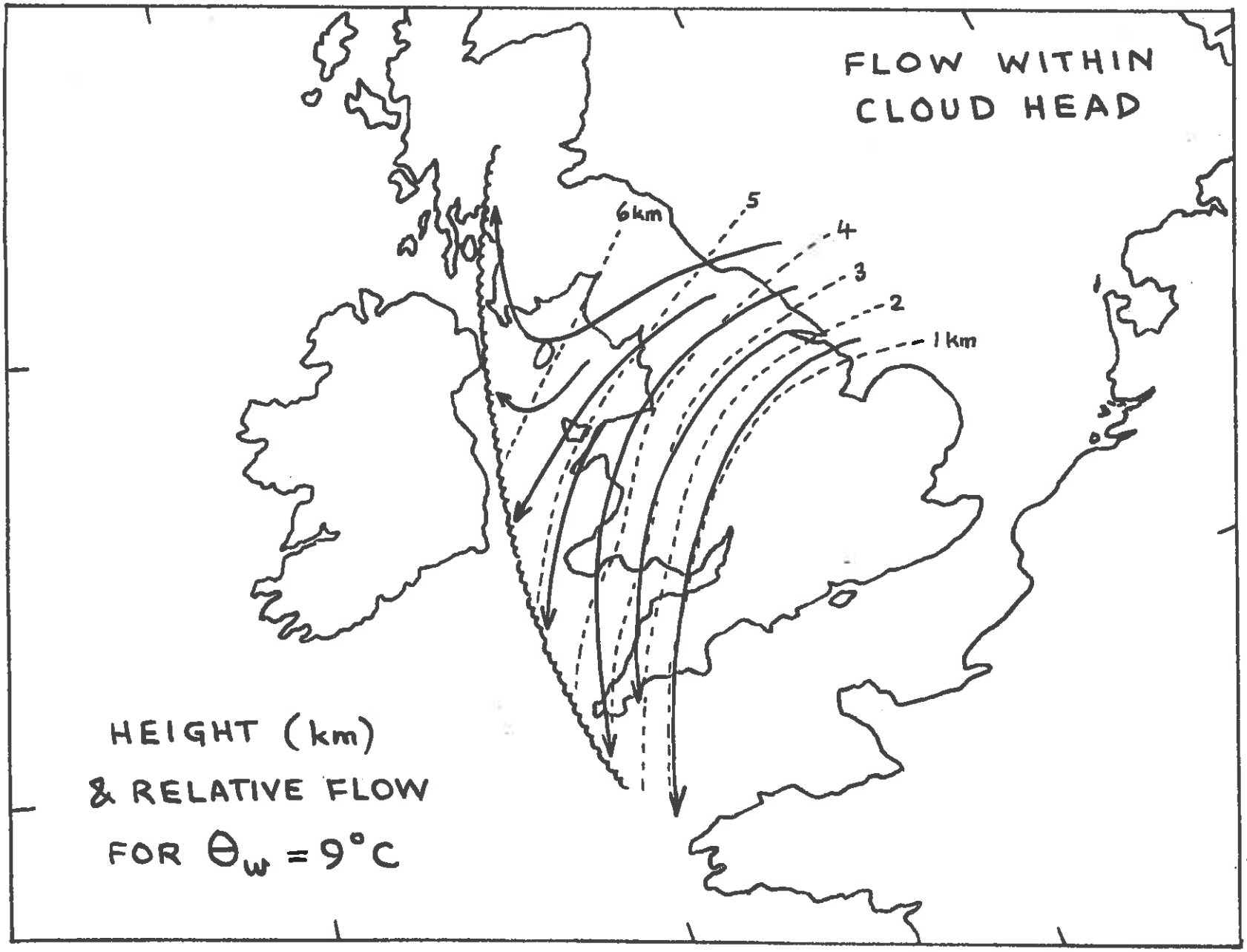
FLOW WITHIN
CLOUD HEAD
6km
5
4
3
2
1km
HEIGHT (km)
& RELATIVE FLOW
FOR $\theta_w = 9°C$

Fig 8(d)

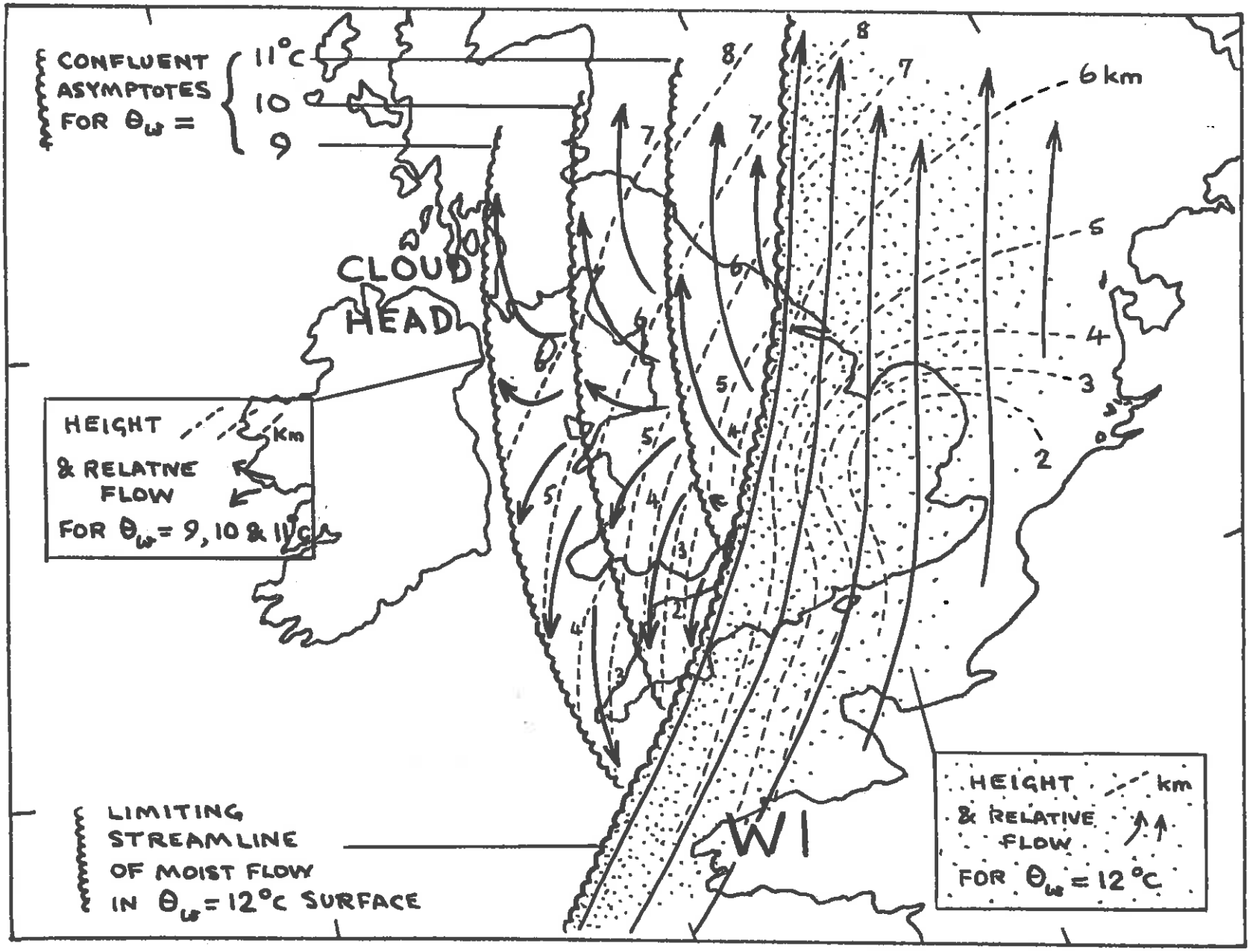
CONFLUENT ASYMPTOTES FOR θ_w =
11°C
10
9
CLOUD HEAD
HEIGHT km & RELATNE FLOW FOR θ_w = 9, 10 & 11°C
LIMITING STREAMLINE OF MOIST FLOW IN θ_w = 12°C SURFACE
WI
HEIGHT km & RELATIVE FLOW FOR θ_w = 12 °C
6 km
8
7
5
4
3
2
1
0

Fig 8(e)

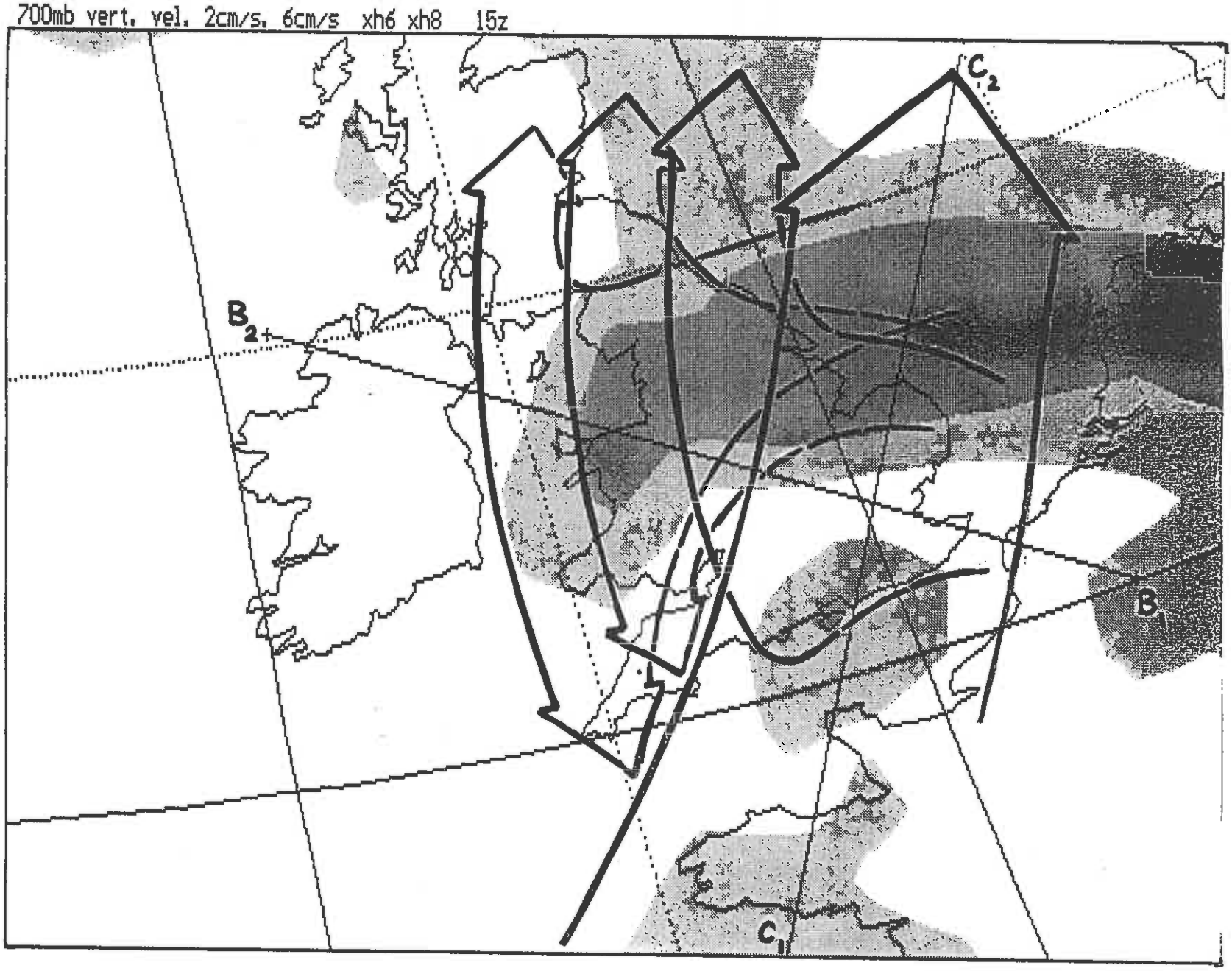

Fig 9(a)

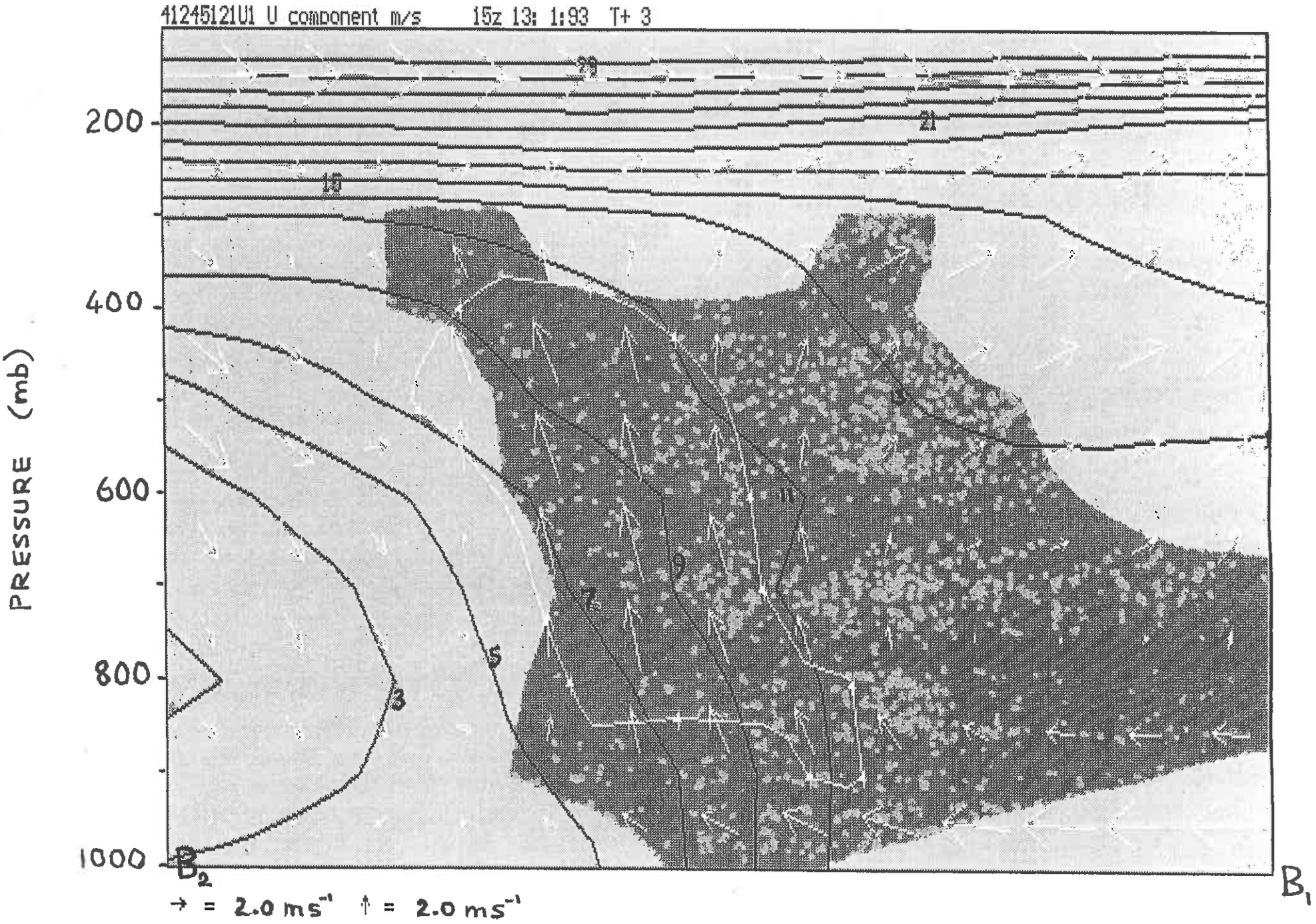
41245121U1 U component m/s 15z 13: 1:93 T+ 3
200
400
600
800
1000
PRESSURE (mb)
B2
B1
→ = 2.0 ms⁻¹ ↑ = 2.0 ms⁻¹

شکل 9(ب)

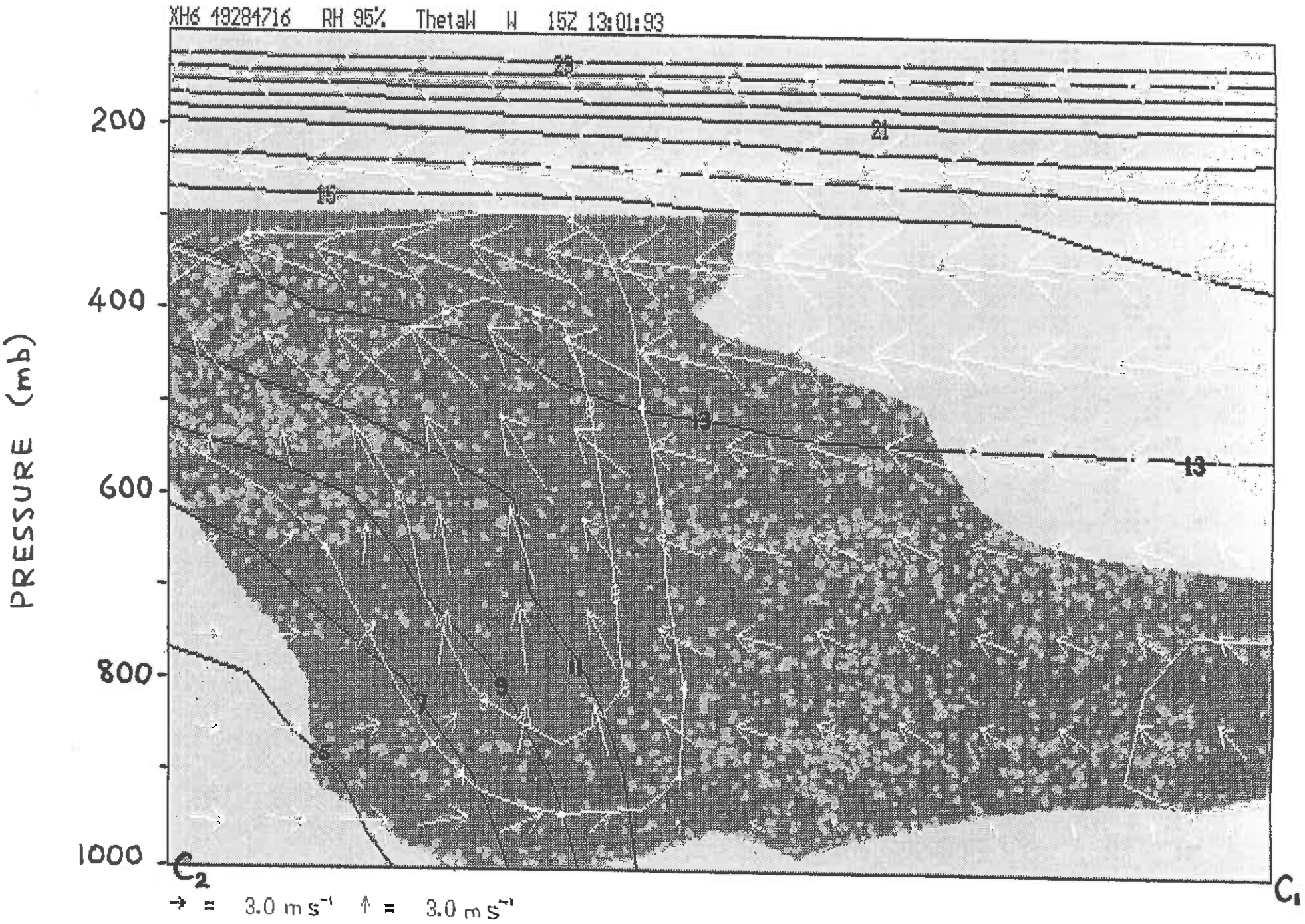
XH6 49284716 RH 95% ThetaW W 15Z 13:01:93
23
21
19
15
13
13
11
9
7
5
200
400
600
800
1000
PRESSURE (mb)
C2
C1
→ = 3.0 m s⁻¹ ↑ = 3.0 m s⁻¹

Fig 9(c)

Fig 10

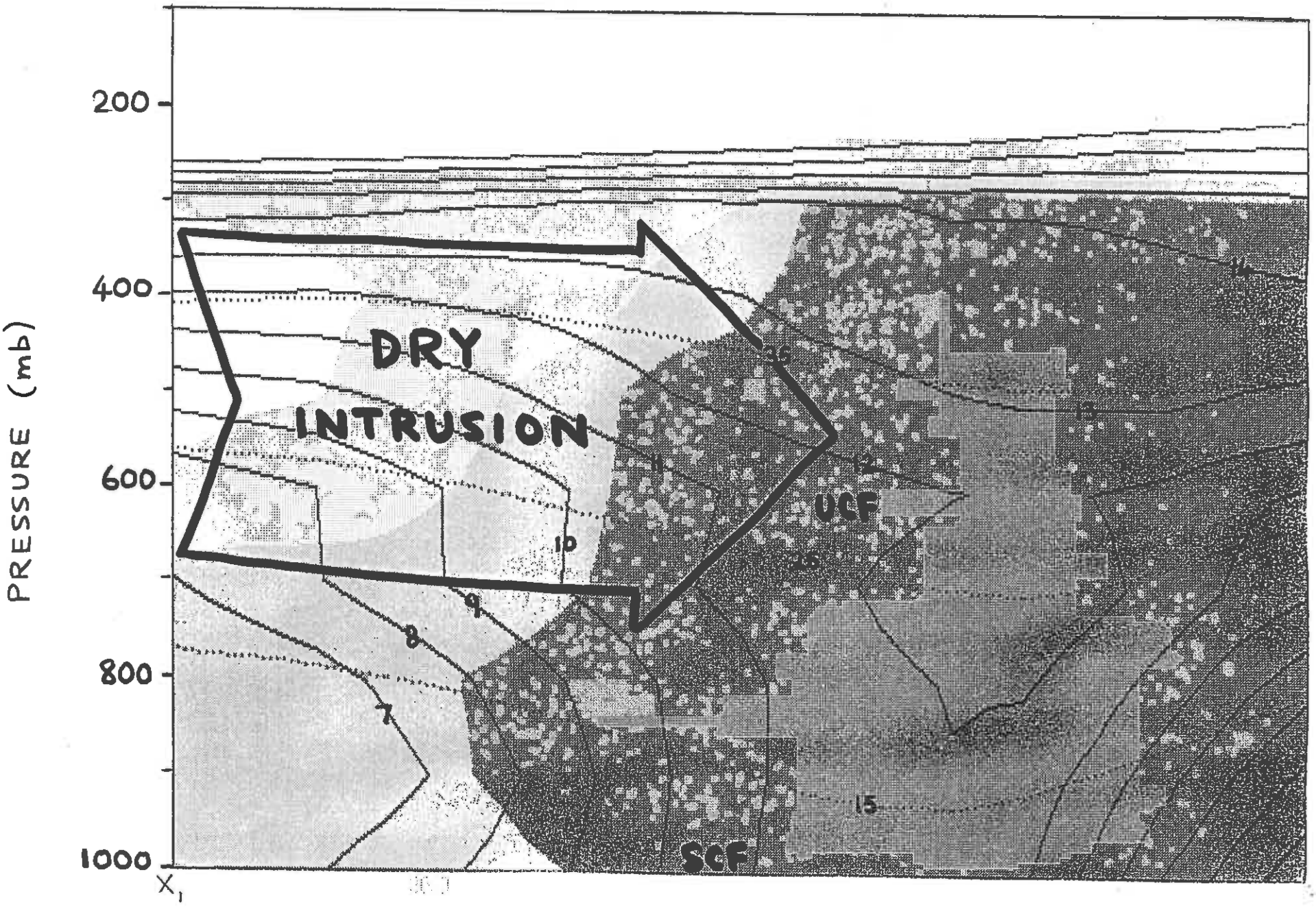
200
400
600
800
1000
PRESSURE (mb)
X_1
DRY
INTRUSION
UCF
SCF
16
14
13
12
11
10
9
8
7
15

Fig. 11

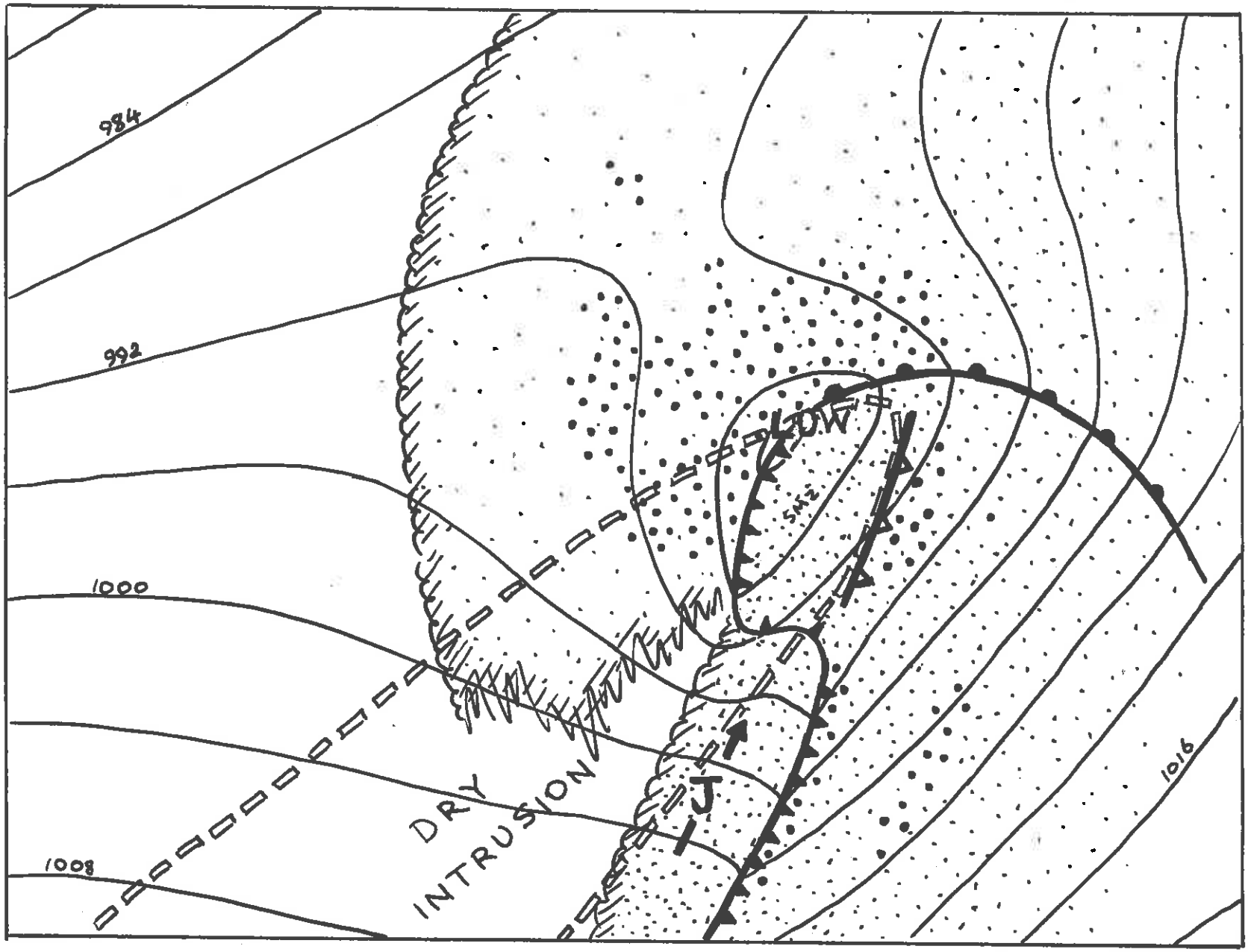

Key to Fig 11: Explanation of the analysis scheme in Fig 11

sea level isobars

edge of major cloud features
(hook cloud, thinly stippled; polar front cloud, thickly stippled: rain, large dots)

boundary of dry intrusion
(the dry intrusion is seen as a dry slot; it overruns a shallow moist zone of higher θ_w and undercuts rear edge of polar front cloud)

surface warm front (cold conveyor belt air ahead of the warm front has a system-relative motion towards the west and contributes to most of the precipitation-producing ascent within the hook cloud).

sharp surface cold front (SCF)
(associated with V-shaped isobars, an abrupt drop in θ_w and narrow line convection)

diffuse surface cold front
(no abrupt changes, no precip., no cloud signature) (the surface cold front in this location may sharpen during the subsequent occlusion process as air from the cold conveyor belt sweeps around the southern flank of the cyclone centre).

upper cold front (UCF)
(marking leading edge of dry intrusion)

300 mb jet axis in the vicinity of its core.

jet core
(in the region of deceleration ahead of J there is an indirect ageostrophic circulation, in which boundary layer air from the warm conveyor belt flows towards the cyclone centre, ascends at the line convection and then forms the top of the eastern part of the hook cloud)

shallow moist zone (SMZ)
(region between the UCF and SCF where moist high-θ_w air in the boundary layer, originating in the warm conveyor belt, is overrun by the lower-θ_w dry intrusion).

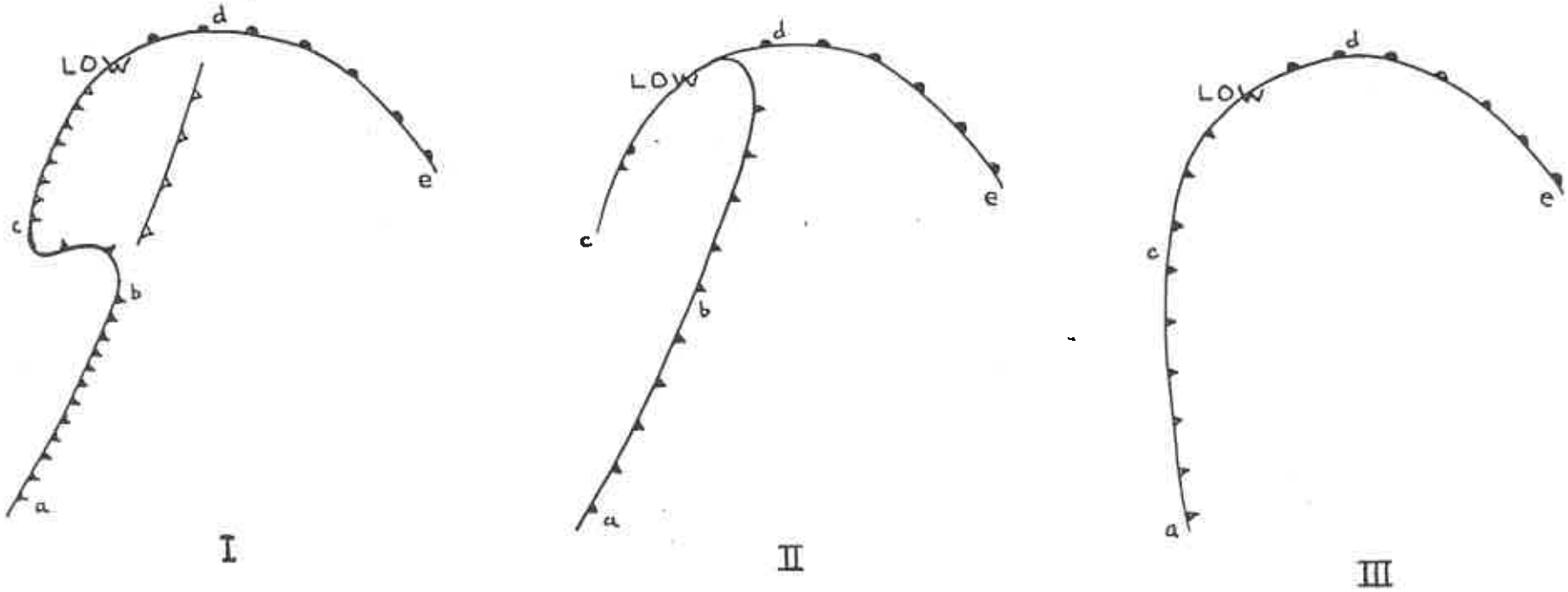

Fig 12

CURRENT JCMM INTERNAL REPORTS

This series of JCMM Internal Reports, initiated in 1993, contains unpublished reports and also versions of articles submitted for publication. The complete set of Internal Reports is available from the National Meteorological Library on loan, if required.

1. **Research Strategy and Programme.**
   K A Browning et al
   January 1993

2. **The GEWEX Cloud System Study (GCSS).**
   GEWEX Cloud System Science Team
   January 1993

3. **Evolution of a mesoscale upper tropospheric vorticity maximum and comma cloud from a cloud-free two-dimensional potential vorticity anomaly.**
   K A Browning
   January 1993

4. **The Global Energy and Water Cycle**
   K A Browning
   July 1993

5. **Structure of a midlatitude cyclone before occlusion.**
   K A Browning and N Roberts
   July 1993

Met Office Joint Centre for Mesoscale Meteorology Department of Meteorology
University of Reading PO Box 243 Reading RG6 6BB United Kingdom
Tel: +44 (0)118 931 8425 Fax: +44 (0)118 931 8791
www.metoffice.com